USE OF STRUT-AND-TIE MODELS TO CALCULATE THE STRENGTH OF DEEP BEAMS WITH OPENINGS

By
Robert Zechmann
and
Adolfo B. Matamoros

Structural Engineering and Engineering Materials
SM Report No. 69

UNIVERSITY OF KANSAS CENTER FOR RESEARCH, INC.
LAWRENCE, KANSAS
July 2002

Acknowledgement

I would like to acknowledge the National Science Foundation for their support throughout my graduate studies and, in particular, during the duration of my work on this special project. The National Science Foundation Graduate Research Fellowship made it possible to devote all of my efforts to the study of this topic and report.

Abstract

Strut-and-tie modeling is a method applicable to almost every design situation in reinforced concrete. This is a behavioral theory proposed as a alternative to past design strategies utilizing empirical formulas and parameters. Since the original presentation of this method in the 60's numerous experimental studies have been conducted, yet the topic of deep beams with large web openings has not been widely covered. Design codes and guidelines also do not commonly cover this topic. However empirical design equations have been proposed based on previous research in the field. An empirical method is presented and the relation to the beam geometry and behavior is discussed. A discussion of the strut-and-tie method is also given including the limited previous research and application of the method.

These two methods are compared using previous experimental results of deep beams with openings. The comparison includes analysis of predicted loads and ultimate loads as well as predicted behavior using the strut-and-tie method for beams with and without web reinforcement. For beams with reinforcement a model was constructed to compare a realistic reinforcement detail. This generates a fairly accurate assessment of strength and behavior with the experimental results. In beams without reinforcement a model is presented using ties only where available. This general model was then adapted to three of the experimental beam geometries. This model gives consistent prediction of the ultimate load and beam behavior in each beam. The results presented reinforce the strut-and-tie method as a safe approach in structurally diverse situations where empirical methods may have a limited range of application.

Table of Contents

List of Figures **Page**

List of Tables **Page**

Notation

a – defined in Figure 5.8

a_1 – ratio of opening width to X, see Figure 2.2

a_2 – ratio of opening height to D, see Figure 2.2

Ac – area of concrete under consideration

A_N – area of node

A_{ps} – area of prestressing steel

A_s – area of reinforcing steel

A_{ST} – area of tie steel

A_w – web reinforcing steel area

B – beam width

b – defined in Figure 5.8

C – concrete strength ratio defined on page 9

d – depth from top to center of reinforcing steel

D – depth of beam

Δfp – change in stress on prestressing steel

e_x – eccentricity to opening centroid from midpoint of direct load path, see Figure 2.2

e_y - eccentricity to opening centroid from midpoint of direct load path, see Figure 2.2

f_c' – design concrete compressive strength

f_{cu} – stress capacity defined page 12

F_{NN} – node capacity

F_{NS} – nominal strut capacity

F_{NT} – strength of ties

fse – prestressing steel stress capacity

f_{sy} – yield strength of reinforcing steel

F_u – strut ultimate capacity

f_u – ultimate stress of steel

f_y – yield stress of steel

h – defined in Figure 5.8

K_1 – ratio of XN to horizontal center of opening, see Figure 2.2

K_2 – ration of D to vertical center of opening, see Figure 2.2

m – length of direct load path

M_{FL} = empirical flexural strength of a deep beam

P_c – concrete shear contribution

P_l – load applied to combined model in beams without reinforcement

P_r – load applied to right portion of model in beams without reinforcement

P_s – shear contribution of bottom reinforcing steel

P_t – total load applied to strut-and-tie model

P_u – ultimate experimental load determined in Kong (1973 and 1977)

P_w – shear contribution of web steel

Q_u – ultimate load from experimental equation given in Chapter 2

w – one half the strut width

W_2 – ultimate load calculated by Kong (1973)

W_u – ultimate load determined from empirical equation given by Kong (1990)

X_N – center to center distance from support to loading point

X_{NET} – defined on page 5

Y_{NET} – defined on page 5

α - angle of reinforcing bars with horizontal

β - angle defined on page 9

β_N – node factor

β_s – strut factor

ϕ - coefficient of cohesion of concrete

ϕ - design resistance factor

λ - lightweight aggregate strength factor

λ_1 – correction factor for opening position within EFGH in Figure 2.1

λ_2 – correction factor for interruption of load path

λ_3 – correction factor for opening size and position

$\rho_s' - A_s/bD$ – reinforcing ratio

ρ_{wt} – web reinforcing steel ratio

ψ_s – empirical constant

ψ_w – empirical constant

Chapter 1 Introduction

Reinforced concrete deep beams are used in many structural applications. Deep beams are common in foundation elements of high-rise buildings, i.e. collector beams, and other structural applications. In some instances it becomes necessary to allow openings in deep beams for HVAC purposes, door and window openings, and other architectural reasons. These openings present unique stress situations that are not widely considered by design guidelines and codes. While design recommendations for deep beams are provided in ACI, CEB-FIP, and BS CP 110 Codes, there is no direct consideration for design of deep beams with openings. In the old CIRIA Code (Ove Arup and Partners, 1977), deep beams with openings are mentioned, but guidelines are based on the available literature and construction practices of the time (Kong 1990). As mentioned by Kong (1990) these guidelines are not significant enough for the design engineer and alternatives should be found.

Empirical equations present an alternative to the suggestions in CIRIA. Kong gives an example of these. These equations were developed to control the most common mode of failure observed in laboratory tests. The validity of these equations is therefore limited to a certain range of geometrical and loading parameters used in the empirical derivation. A review of a common empirical design alternative is presented.

A second alternative for design has been the use of strut-and-tie models. Strut-and-Tie modeling is suitable for use in a wide range of design problems and is slowly being incorporated into most design codes and guidelines across the world.

Among others, it can now be found in the EuroCode 2, FIP Recommendations (CEB-FIP 1996.), and Appendix A of ACI 318-02 (2002). A review of the strut-and-tie approach and some experimental background for deep beams with web openings is presented.

The use of strut-and-tie modeling allows the structural engineer increased control over the design process. These models can be used with confidence in situations where the empirical equations lose validity. The models can also be adapted from a general model for beams with a web opening to a specific geometry with consistency.

Limited results were available for beams with openings and specific configurations of web reinforcement. One set of tests were run by Kong (1977) in which differing reinforcement layouts were tested while controlling the opening orientation and size. Results from a strut-and-tie model are presented and compared with these experimental results. In addition, two other models and a supplementary design problem are presented to give examples of adapting strut-and-tie models to similar but significantly different beam geometries.

Kong (1973 and 1977) compiled much data on the behavior of beams without web reinforcement and this data will be used to show the relation of the general model in specific cases. Three models are presented that have been adapted from a general model describing the behavior of these beams. Each beam has a different opening orientation to show any trends in using the strut-and-tie models.

Chapter 2 Empirical Design Equations

The empirical equations presented in Kong 1990 were developed from observation of test specimens. Hundreds of test specimens with varying opening size, opening position, and loading scheme were tested to failure (Kong 1990). From this finite number of tests, the observed behavior was used to develop design requirements and recommendations. Since these recommendations originate from experimental results, the design parameters of the specimens define a large number of inherent design variables.

Parameters applied to these recommendations have been simplified by the following assumptions (Kong 1990):

(i) the effect of the opening lying only within the region EFGH (practical region) in the web of the deep beam is considered (Figure 2.1);

(ii) the size of the opening is limited to $a_1x \leq x_N/2$ and $a_2D \leq 0.3D$, as shown in Figures 1.2.

(iii) the eccentricities e_x and e_y of the opening are limited to the maximum of $X_N/4$ and $0.6D/4$ in the X- and Y- directions respectively (Figure 2.2).

With these parameters in mind the behavior of the ultimate strength is described through applying three factors to the solid web equation. The position of the opening within the region EFGH adjusts the ultimate strength by the factor λ_1:

$$\lambda_1 = \left[1 - \frac{1}{3}\left(\frac{K_1 X_N}{K_2 D}\right)\right] \quad for \quad \frac{K_1 X_N}{K_2 D} \leq 1$$

$$\lambda_1 = \frac{2}{3} \quad for \quad \frac{K_1 X_N}{K_2 D} \geq 1$$

An opening positioned such that the centroid is further away horizontally from the loading zone than vertically will reduce the strength by 2/3. This accounts for failure similar to the diagonal slip type in a solid deep beam. These failures are affected by the shear span to depth ratio used in the λ_1 equation.

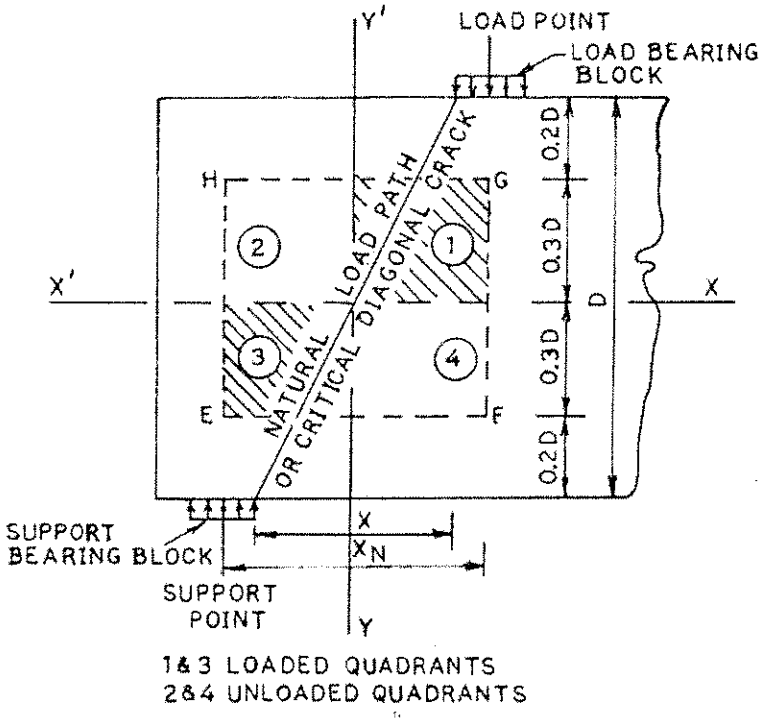

Figure 2.1: Useful region limiting location of openings for empirical equation.

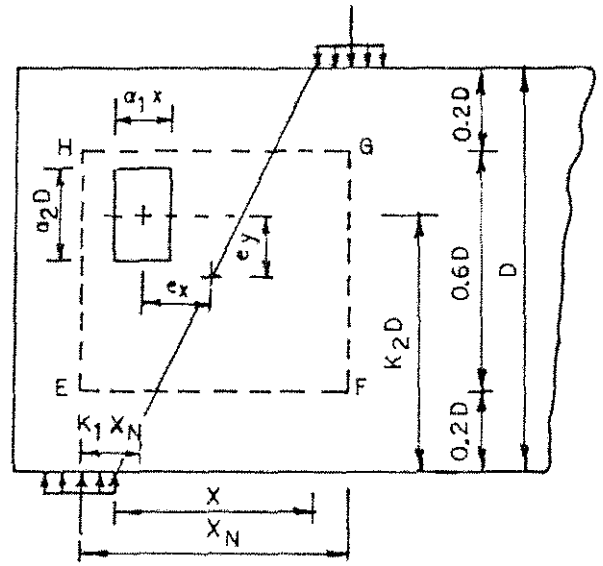

$X_{net} = (X_N - a_1 X)$
$Y_{net} = (0.6D - a_2 D)$
$e_x \leq X_N/4$
$e_y \leq 0.6D/4$

Figure 2.2: Limitations of web openings and representation of equation variables.

The disruption of a direct load path from the applied load to the support also changes the ultimate strength of a deep beam. The strength shall be reduced by the factor λ_2 where $\lambda_2 = (1-m)$ and m is the ratio of the intercepted path length to the total path length. Therefore, the greater length of the direct load path occupied by a void the lower the ultimate strength will be.

The size and location of the opening is accounted for by the factor λ_3. Where

$$\lambda_3 = \left[0.85 \pm 0.3\left(\frac{e_X}{X_{net}}\right)\right]\left[0.85 \pm 0.3\left(\frac{e_Y}{Y_{net}}\right)\right] \text{ and}$$

$$e_X \leq X_N/4 \quad e_Y \leq 0.6D/4$$
$$X_{net} = (X_N - a_1 x) \quad Y_{net} = (0.6D - a_2 D)$$

When the given eccentricity limitations are not meet Figure 2.3 may be used to calculate working eccentricities for use in calculating λ_3.

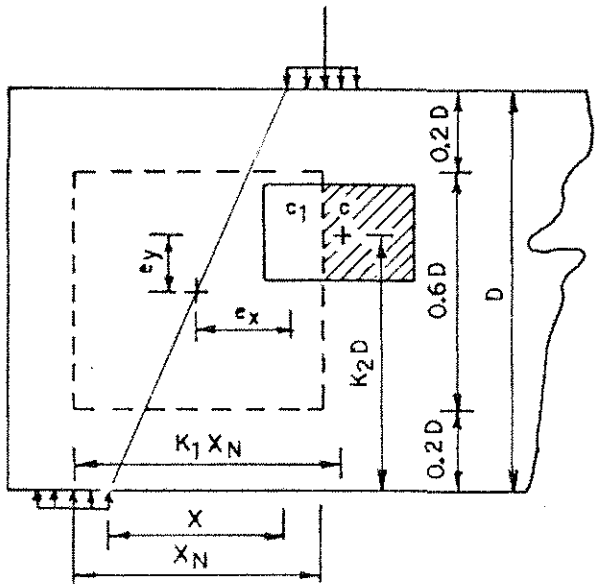

Figure 2.3: Eccentricity parameters when opening extends beyond web limitations.

The factor λ_3 is limited by 0.5 and 1 depending on location of the opening in a loaded or unloaded quadrant. Quadrants 1 and 3 are the loaded quadrants and 2 and 4 are the unloaded quadrants as seen in Figure 2.1. The negative sign is used when the opening falls within 1 or 3, thus reducing the strength. The positive sign may be used when the opening falls within 2 or 4.

As shown by Kong (1990), the main mode of failure for deep beams with openings is shear. An inclined crack extends from two of the web opening corners to both the loading and support zone. Cracks such as 1 and 2 from Figure 2.4 are examples of these. In numerous test results form Kong (1982 and 1990) these crack patterns were consistent. A crack originates in the center of the region between the

opening edge and the loading or the support edge. These cracks continue to propagate diagonally until they span the distance from the loading pad and/or support pad to the opening edge. It was observed that the exact location of the crack on the opening depends on the loading scheme, opening position, opening size, and opening shape. This behavior holds true for openings that are found in the shear zone and openings that alter the load path in the deep beam. The results showed that deep beams with openings carry loads less efficiently than regular deep beams and the design factors previously mentioned account for this behavior.

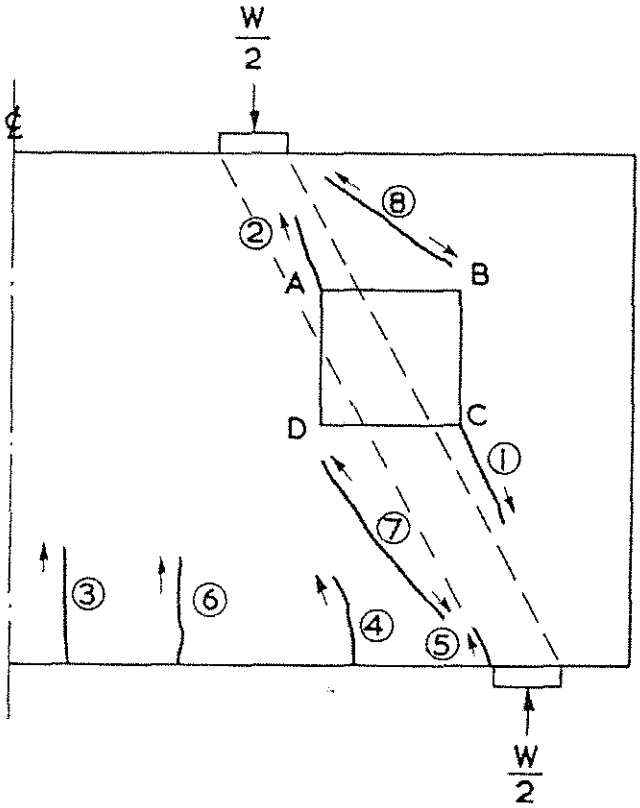

Figure 2.4: Typical crack pattern in a deep beam with opening.

Generalizations about reinforcement layouts were made in Kong (1977). The maximum shear strength of deep beams with openings was achieved with steel reinforcement oriented diagonally above and below the openings. The second best performance was found with horizontal web reinforcement accompanied by minimal amounts of vertical reinforcement. It was also mentioned that with deep beams the horizontal tension reinforcement contributes greatly to the ultimate shear strength and this is reflected in the ultimate shear equation derived in Kong (1990).

The ultimate shear equation given by Kong (1990) is based on shear resistance components of a solid deep beam associated with the concrete, the tension reinforcement, and the web reinforcement. The effect of web openings is accounted for through constants, λ_1, λ_2, and λ_3, to the concrete shear strength, P_c as described earlier. The equation is as follows:

$$Q_u = P_c(\lambda_1 \times \lambda_2 \times \lambda_3) + \psi_s P_s + \psi_w P_w$$

where $P_c = \dfrac{cbD}{\sin\beta\cos\beta(\tan\beta + \tan\phi)}$ $P_s = F_s\left[\dfrac{\tan\beta\tan\phi - 1}{\tan\beta + \tan\phi}\right]$

$$P_w = F_w\left[\frac{\sin\alpha\cos\beta + \cos\alpha}{\left(\dfrac{\tan\beta + \tan\phi}{\tan\beta\tan\phi}\right)} - \frac{\cos\alpha}{\left(\dfrac{\tan\beta + \tan\phi}{1 - \tan\alpha\tan\beta}\right)}\right]$$

and

$$\lambda_1 = \left[1 - \frac{1}{3}\left(\frac{K_1 X_N}{K_2 D}\right)\right] \quad for \quad \frac{K_1 X_N}{K_2 D} \le 1$$

$$\lambda_1 = \frac{2}{3} \quad for \quad \frac{K_1 X_N}{K_2 D} \ge 2$$

$\lambda_2 = (1-m)$ m = path length intercepted to natural unintercepted path

$$\lambda_3 = \left[0.85 \pm 0.3\left(\frac{e_S}{X_{net}}\right)\right]\left[0.85 \pm 0.3\left(\frac{e_e}{Y_{net}}\right)\right]$$

$$e_S \le X_N/4 \quad e_Y \le 0.6D/4$$
$$X_{net} = (X_N - a_1 x) \quad Y_{net} = (0.6D - a_2 D)$$

$$c = \sqrt{f_c' f_t'}/2 \quad \tan\phi = (f_c' - f_t')/2\sqrt{f_c' f_t'}$$

ψ_s = is an empirical coefficient = 0.65

ψ_w = is an empirical coefficient = 0.5

b = beam width

D = depth

β = angle of inclination of rupture plane with horizontal

α = angle of inclination of inclined web bar with horizontal

see Figures 2.1 – 2.3 for other definitions

It is apparent that the above equation is complex and it has been simplified for design purposes. The simplified design equation is:

$$Q_u/bD = 0.1 f_c'(\lambda_1 \times \lambda_2 \times \lambda_3) + 0.0085\psi_s p_s f_{sy} + 0.0085\psi_w K_w r_w f_{wy}$$

where $p_s = A_s/bD \times 100 \quad r_w = \sum A_w/bD \times 100 f_{wy}$

An empirical flexural design strength equation was also developed for solid beams:

$$\frac{M_{FL}}{bd^2 f_c'} = \frac{p_s' f_{sy}}{f_{sy}'}(0.86) + \frac{p_{wt} f_{wy} \cos\alpha}{f_c'}(0.52) + 0.033$$

$$p_s' = A_s/bD \quad p_{wt} = \sum A_w/bD$$

This equation does not account for openings and shouldn't be used for design of deep beams with large openings.

Design guidelines to accompany these equations were given by Kong (1977).

1.) Web openings should be kept clear of natural load path. If the opening is reasonably clear of the load path the unadjusted shear strength can be used.
2.) Web openings should be protected above and below opening with web reinforcement to increase the shear capacity of the deep beam.
3.) Trimming the web opening with reinforcement does not increase the shear capacity of the deep beam.
4.) Inclined web reinforcement is very effective for increasing the ultimate shear strength of the deep beam.

Using these guidelines and equations the engineer can develop designs for a limited number of loading situations.

Ch 3 Strut-And-Tie Modeling

In contrast to the empirically derived equation, a strut-and-tie model is a powerful design resource that can be used in virtually any structural concrete application. Deep beams with web openings are the same as any other strut-and-tie problem and the strategy is as follows from Schlaich (1987):

- Define D and B regions as shown in Figure 3.1.
- Construct the optimal truss model to resemble the flow of forces in the structural element.
- Design reinforcing ties based on tensile strength of bars.
- Check the nodal concrete stresses and anchorage lengths.

By following the second step closely, strut-and-tie modeling is a lower bound solution. This is achieved by orienting the truss model with respect to the elastic stress fields and designing for plastic strength behavior (Schlaich 1987). This procedure will provide a safe and serviceable structure under design loads as shown in experimental studies.

Step three and four are the steps in which plastic strength behavior is used to insure proper strength behavior of the struts, ties, and nodes. Strength calculations for the struts, ties, and nodes are fairly consistent among design codes. CEB-FIP Recommendations (1996) and ACI 318-02 (2002) are examples of design codes that allow the use of Strut-And-Tie models. These account for design conditions using the same equations with exception to notation and minor differences in safety factors.

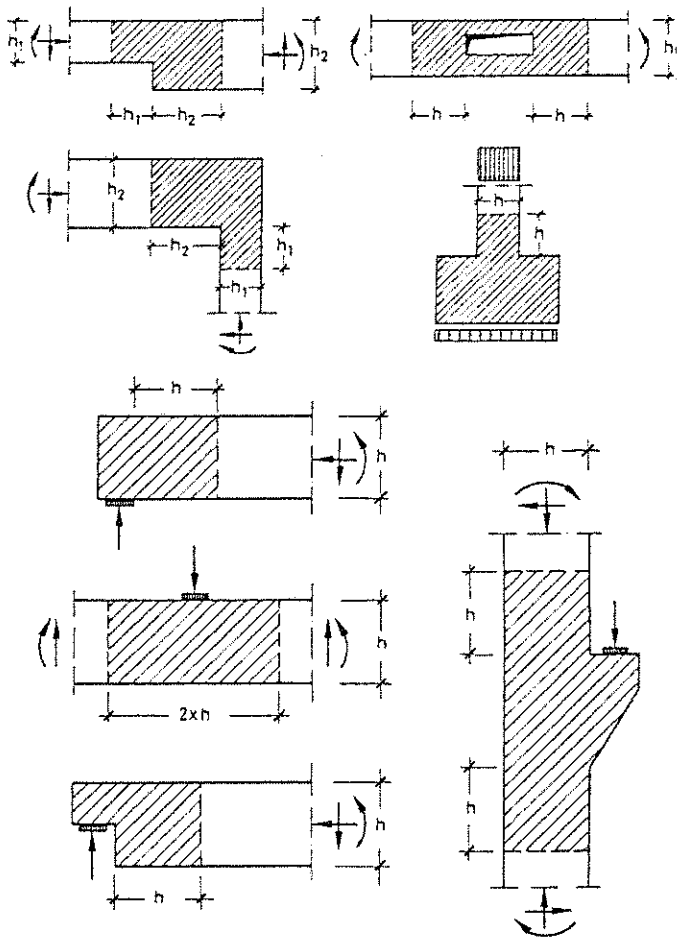

Figure 3.1: Definition of typical D regions (shaded) and B regions (non shaded).

The design strength of struts, ties, and nodes for steps three and four can be determined using the ACI 318-02 equations. The strength for struts is described by:

$$F_u \leq \phi F_{ns} = \phi f_{cu} A_c \text{ where } f_{cu} = 0.85\beta_s f_c'$$

β_s depends on the type of concrete strut, i.e. the shape of the stress field, and ranges from 1.0 for a uniform strut to 0.4 for a strut in a tension member or flange. Compression reinforcement may also be used to increase the strength of a strut as

given in ACI 318-02. The strength of the reinforcement ties is determined from the following equation:

$$F_{nt} = A_{st}f_y + A_{ps}(f_{se} + \Delta f_p)$$

Where A_{ps} is zero for nonprestressed members and special attention should be given to ensure proper anchorage of reinforcement. The strength of nodes is determined using the following equation:

$F_{NN} = f_{cu}A_N$ where

A_N is the proper area determined from ACI 318-02 within the nodal zone.

$f_{cu} = 0.85\beta_n f_c'$ where

β_n is determined by the type of node, i.e. the type forces involved

$\beta_n = 1.0$ for nodes bounded by compression forces

$\beta_n = 0.8$ for nodes including one tie

$\beta_n = 0.6$ for nodes including two or more ties

Some experimental work using strut-and-tie models on deep beams with web openings has been done. Maxwell (1996) gives an example of applying strut-and-tie models to deep beams with openings. This example presents different failure modes for differing strut-and-tie models applied to the same structural system. The failure of each beam could be traced to the weak points of each model and the reinforcement layout. These tests showed successful prediction of load carrying behavior according to the reinforcement layout chosen and the predicted to ultimate load ratio ranged from 0.52 to 0.71.

Cracking patterns shown in Figure 3.2 were consistent with the load carrying mechanism defined by the strut-and-tie layout and the general assumptions for deep beam behavior. Although, one of these models is contradictory to the assumed mode of failure based on empirical equations. This was observed in the third specimen tested by Maxwell (1996) seen in Figure 3.2c. Failure occurred at the center lower node of the beam. This contrasts the assumption used in the empirical design that beams will fail in shear passing through the web openings. Failure occurred due to large compressive stresses at the center lower node.

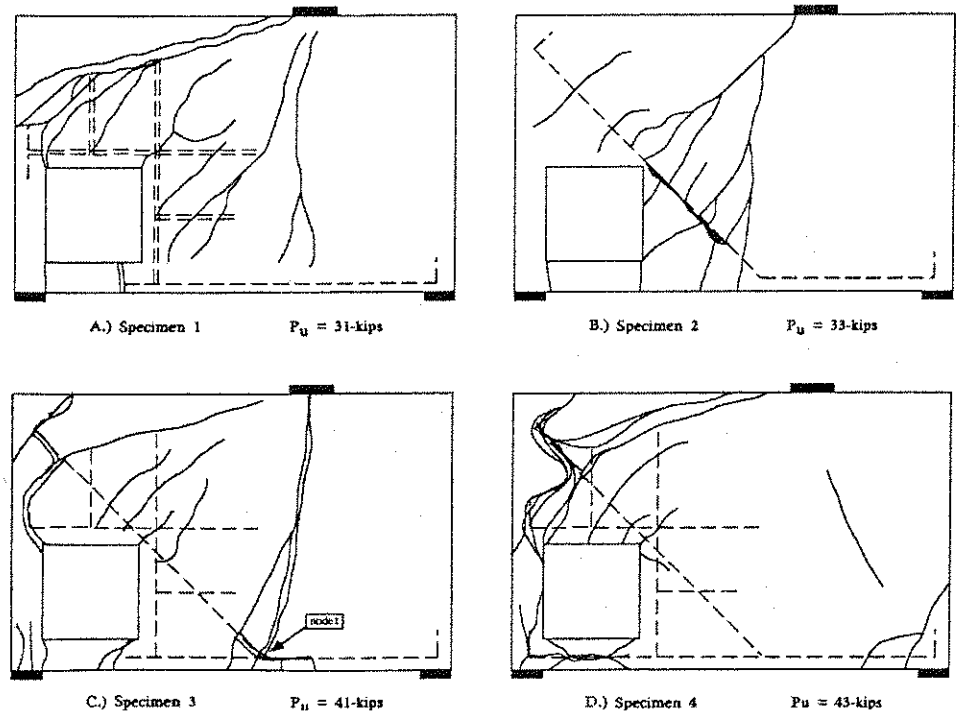

Figure 3.2 Deep beams with openings and the corresponding crack patterns. (Maxwell 1996)

Maxwell observed increased control over the behavior of the test beams in the region below the web opening. In two of the four specimens the center portion was not reinforced due to load carrying assumptions. In these beams the portion below the

opening cracked first and transferred no load while the load carrying regions successfully transferred the design loads. This behavior would not be specifically predicted by an empirical equation. These examples given by Maxwell (1996) show that cracking behavior and ultimate failure relate well to the assumptions made in the strut-and-tie approach to modeling.

Chapter 4 Deep Beams with Openings with Web Reinforcement

Kong (1973 & 1977) constructed and failed 7 types of deep beams with various reinforcement configurations (Figure 4.1). These beams had identical geometric properties in overall size and web opening. The reinforcement ratio was held constant while the reinforcement layout was varied to compare the efficiency.

The increase in ultimate strength with respect to an unreinforced reference beam, shown in Table 4.1, ranges from 154% to 317%. From these results it is obvious as stated earlier that using the W6 and W4 inclined reinforcement layout will yield the greatest ultimate load with a constant reinforcement ratio. W7, having the second best result, uses vertical reinforcement and will be addressed with a supplemental example problem given in Appendix C. W3 achieved the next best ultimate load increase of 215% using horizontal reinforcement.

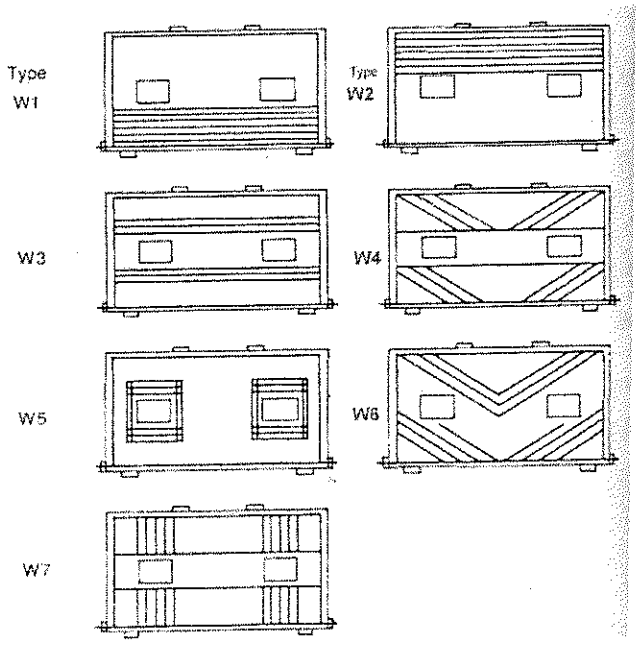

Figure 4.1: Reinforcing layouts for experimental beam specimens.

Table 4.1: Experimental Results attained by Kong (1977)

Beam	Ultimate Load (kN)	Percent Increase w/ Reinforcement
W6-0.3/4	825	317%
W4-0.3/4	660	254%
W7-0.3/4	630	242%
W3-0.3/4	560	215%
W2-0.3/4	490	188%
W1-0.3/4	400	154%
W5-0.3/4	370	142%
O-0.3/4	260	100%

4.1 General Model Development

A dependable relation in terms of reinforcing layout and strut-and-tie layout can be determined using results from Kong (1977) and engineering analysis. In most cases for constructive ease reinforcing should be oriented orthogonal to the beam layout. Therefore, although beams W6 and W4 give the highest ultimate load, they are not the best choices for design. This leaves W1 through W3, W5, and W7 for consideration as a design option. W7 uses orthogonal reinforcement and would make a good selection, although quantifiable results were not attainable from the experimental report. W3 uses constructively simple horizontal reinforcement placed the length of the beam above and below the opening and has quantifiable reinforcement from the experimental report. W3 being an idea use of steel with the next highest ultimate load is therefore the best selection for a strut-and-tie relation.

In contrast to the W3 layout, the W5 layout provides horizontal reinforcement in the same vertical position yet, does not extend the bars the length of the beam. The

reinforcing bars in W5 are terminated shortly past the opening, as seen in Figure 4.1. The test results show that this is indeed a poor design detail. Even though W5 had more tie capacity concentrated above and below the opening, the ultimate load for W5 was only 66% of W3. Most likely there was not enough anchorage to develop the total strength of the reinforcement. In support of this, the cracking patterns shown in Figure 3.2 show more intense cracking damage under less load near the areas of bar termination in W5 compared to the same area in W3.

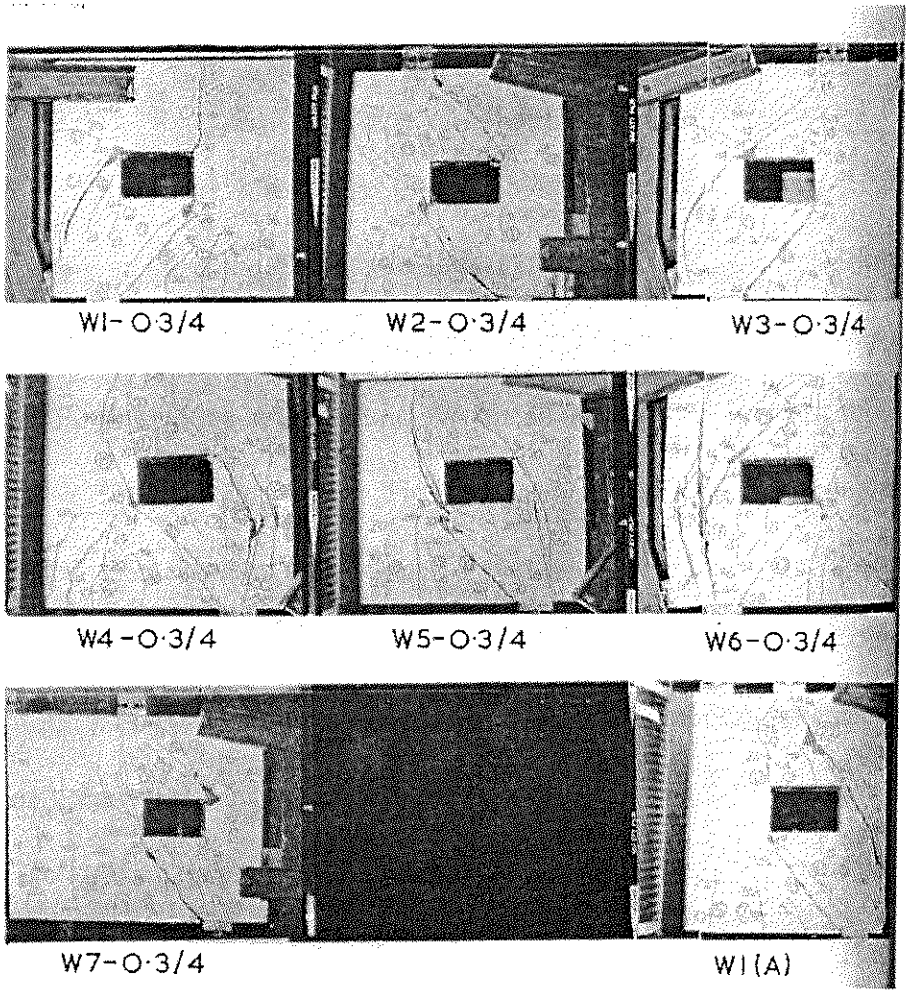

Figure 4.2: Cracking patterns for beams with reinforcement.

Model B was developed using principles for the strut-and-tie modeling of a standard wall opening. The classic example shown by Schlaich (1991) is for a distributed load that must circumvent the opening. This model includes symmetric reinforcement above and below the opening as seen in Figure 4.3. Using this idea the model for beam W3 uses symmetry about a direct load path from load pad to support shown in Figure 4.4. The upper horizontal tie is extended beyond the opening to the left and made symmetric about the path. The top bar is then copied and placed underneath the opening to create a mirror of the upper truss. This provides a quick solution to the entire model since upper and lower forces mirror each other.

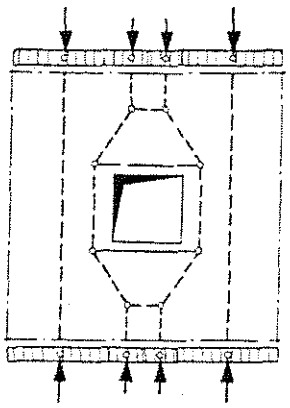

Figure 4.3: Strut-and-tie model for opening in wall under distributed load. (Schlaich 1991)

The ties and reinforcing steel are oriented in the same direction and located in the same area just as would be done in a design problem. The W3 layout also gives ample room for development of the horizontal tie strength by extending the bars the length of the beam.

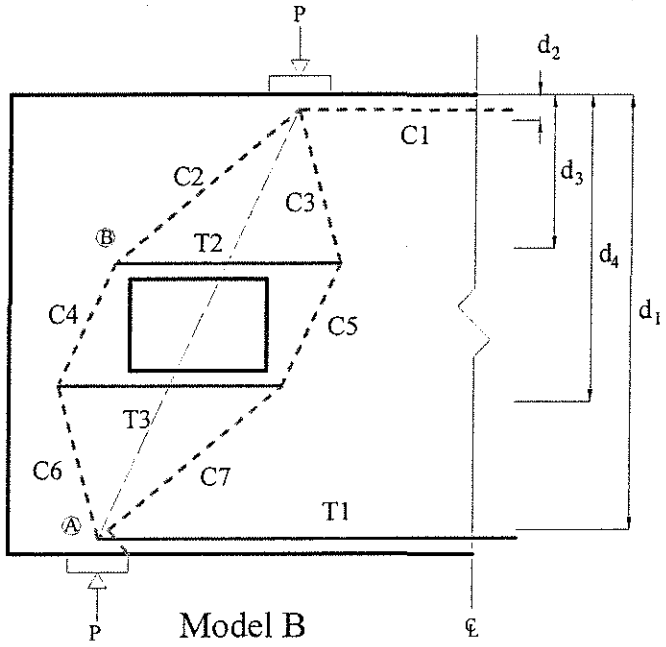

Figure 4.4: Model B strut-and-tie relation to beam W3.

4.2 Forces, Ultimate Load Requirements, and Results

The strut and the tie forces of Model B correlate very well with the concrete and reinforcing capacities for beam W3. The limit for the horizontal tie force is governed by the amount of steel. Kong does not specify a reinforcement cross-section therefore an approximate value was calculated using the volumetric reinforcement ratio given and an estimate of the total reinforcement length. The strut and the nodal capacities were considered at the hydrostatic nodes A and B using the distance from the support edge or the opening corner perpendicular to the strut. The nodal stress limits were calculated using the aforementioned ACI nodal equation:

$f_{cu} = 0.85\beta_n f_c'$ where

$0.85f_c' = f_c'$ from Kong (1973) and

$\beta_n = 0.8$ for nodes including one tie

The strut stress limits were calculated using the similar ACI equation:

$f_{cu} = 0.85\beta_s$ where

$0.85f_c' = f'_c$ and

$\beta_s = 0.6\lambda =$ where $\lambda = 0.85$ for lightweight concrete $\beta_s = 0.6(0.85) = 0.51$

The strut stress will govern due that β_s is smaller than β_n and the same area will be used in both the nodal and strut allowable stress calculations. The following equation was used for the allowable force calculation F_c in kN:

$F_c = \beta_s f_c' \cdot b \cdot 2w \cdot 10^{-3}$ where b = beam width (mm)

w = perpendicular distance to edge (mm), (½ total width of strut)

The strut and the tie capacities are summarized in Table 4.2. These show that strut C2 at Node B controls the design. MathCAD was used to setup the truss calculations and these are given in Appendix A. The ultimate load calculated using C2 as the governing strut is 254 kN, 91% of the 280 kN ultimate load.

Table 4.2: Strut-and-Tie Capacities and Calculated Truss Forces

Node	Strut	Width w (mm)	F_c (kN)	S & T Force, F (kN)	F/F_c
A	C7=C2	50.6	174	153	0.88
B	C2	44.6	**153**	**153**	**1.00**
B	C4	46.3	159	105	0.66

Tie	Yield Strength F_y (kN)	S & T Force (kN)	F/F_y
T1	135	114	0.84
T2	241	91	0.38

This model is further supported by the cracking pattern for W3 in Figure 4.2. There is excessive cracking at node B located at the upper left edge of the opening. As well, there is virtually no tension cracking around the low stressed area of T2 and there is moderate cracking around the moderately stressed area of T1. Based on both numerical analysis and observed behavior, Model B is a good match to beam W3.

4.3 Additional Model Application

As stated earlier, the behavior of a deep beam with an opening will depend on the position and size of the opening and design can be adjusted to account for this. Model C and D shown in Figures 4.5 and 4.7 are examples of adjusting to different openings by applying strut-and-tie models. The openings in Models C and D are very close to the support and would present a tricky design situation without the use of strut-and-tie modeling.

Model C was developed using engineering judgment and an elastic stress vector plot. The elastic stress vectors shown in Figure 4.6 were used as a guide to determine the most logical placement of ties around the opening. Model C is similar to Model B aside from the elastic vector plot and the load path passes through a corner of the opening instead of the center. Carrying compression from the right side of the opening directly to the support is not feasible due to small the angle. A beam like construction could be constructed from node E to D to transfer this load in shear but the area is tight and would be very congested. Instead, using the vertical tie, T4, the load is transferred up to C2, over the opening, and down to the support. The strut-and-ties force calculations for an applied load comparable to Model C are given in

Appendix A and summarized in Table 4.3. As expected C2 and C4 carry the largest strut force while T3 carries the largest tie force. This is due to the addition of the right load carried by T4. The purpose of T2 is to provide crack control in the region beneath the opening at service loads.

Table 4.3: Truss Forces for Model C

Member	Force (kN)	Member	Force (kN)
C2	331	T3	133
C4	284	T1	130
C5	136	T4	107
C1	130	T2	45
C3	117		

Model D is another example where the opening is in a precarious position near the support, yet in this situation the opening is not large. As shown in Figure 4.7 the direct load path between nodes A and E passes near the center of the opening and will allow for a symmetric model. The elastic stress vector plot, Figure 4.8, is also used as a guide in developing model D shown in Figure 4.7. It reinforces a more symmetric stress flow around the opening.

This is an example where a simple strut-and-tie solution can be quickly found but has several drawbacks. Angle $\theta 1$ must be kept above the limit of 25°, and inclined ties are necessary. As mentioned earlier this is not the best alternative for construction. At the expense of longer calculations, a more elaborate model could be developed. One solution could be similar to model C, to redistribute the load above the opening and use orthogonal reinforcement.

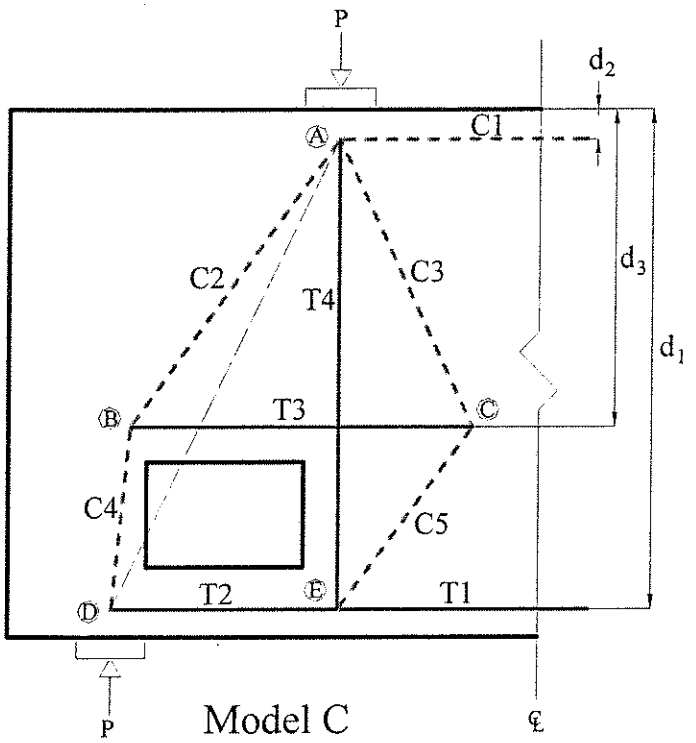

Figure 4.5: Strut-and-Tie Model for beam with a low and wide opening.

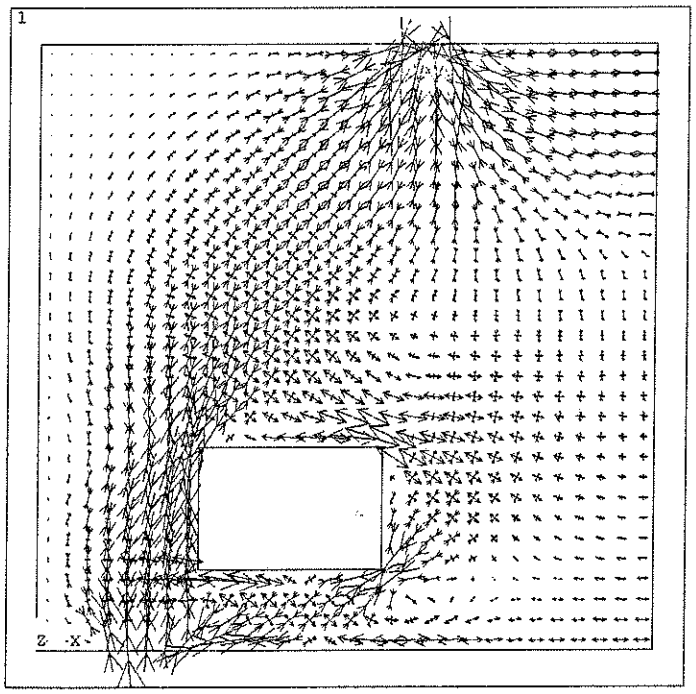

Figure 4.6: Elastic stress vectors used as guide for constructing Model C.

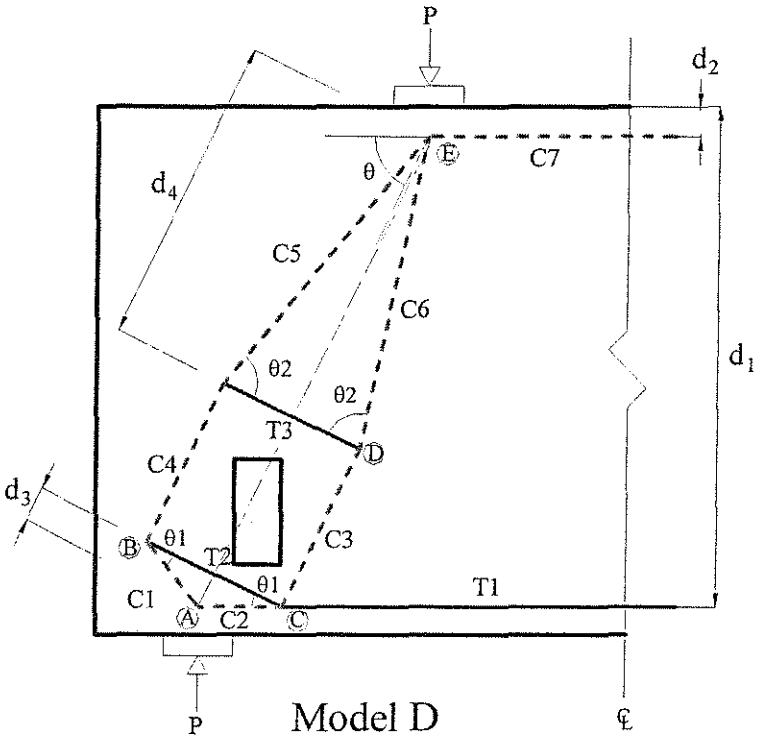

Figure 4.7: Strut-and-tie model for low and narrow opening.

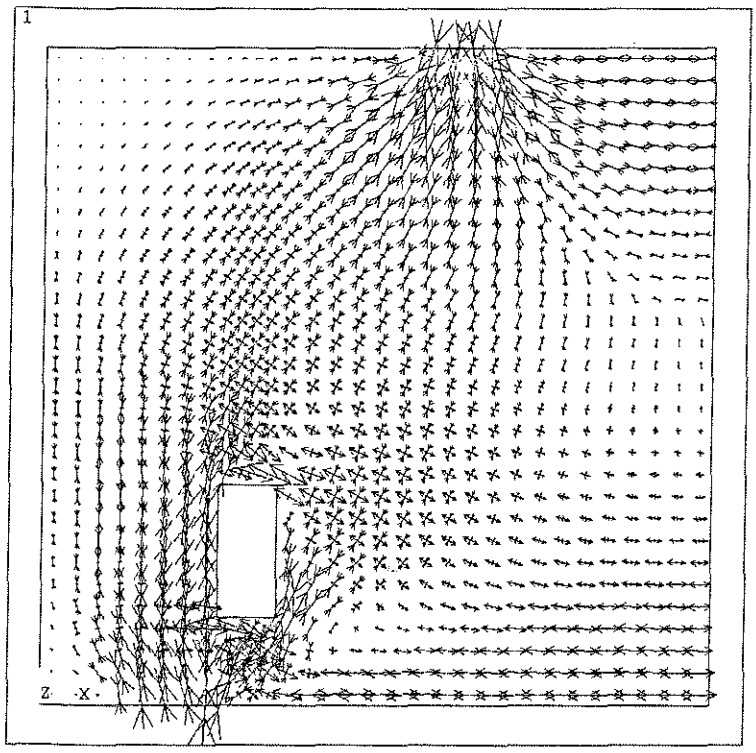

Figure 4.8: Elastic stress vector plot for beam with a low and narrow opening.

Chapter 5 Deep Beams without Web Reinforcement

Another means to assess strut-and-tie modeling for beams with openings is to compare the remaining results published by Kong with a developed model for beams without reinforcement. In researching the behavior of deep beams with openings Kong (1973& 1977) used a combined 32 beams without web reinforcement. The ultimate load and cracking patterns reported for these beams provides a basis to compare the ability of strut-and-tie modeling to predict the behavior and failure load.

Beams O-0.4/2, O-0.4/4, and O-0.4/5 shown in Figure 5.1 will be used in the analysis. It was found that minimal reinforcement was provided outside of the beam web. This is shown in Figure 5.2 given by Kong (1973). The reinforcing scheme used one 6 mm diameter bar around the perimeter of the beam and one 20 mm diameter bar placed near the bottom of the beam and anchored by external blocks. The yielding stress of the bars was 425 N/mm^2 and 430 N/mm^2, respectively. Small reinforcing cages were also placed in the loading and support regions as seen in reinforcement layout shown in Figure 5.2. These were placed to increase capacity against premature local bursting observed in previous experiments.

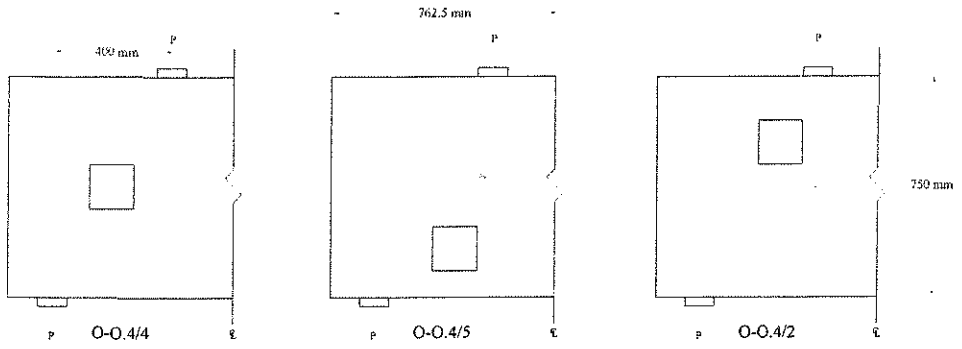

Figure 5.1: Beam configurations for analysis without reinforcement.

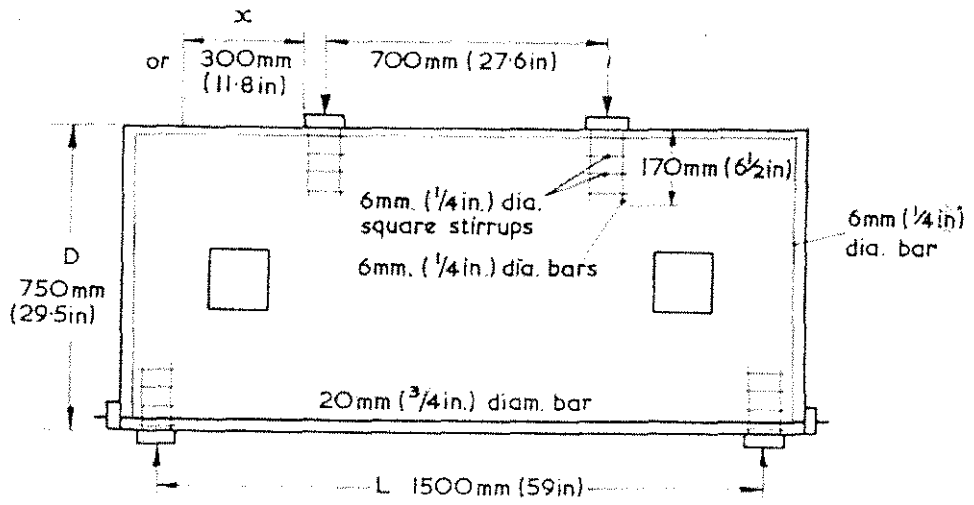

Figure 5.2: Reinforcing scheme for beams without web reinforcement (Kong 1973).

5.1 General Model Development

The models for a beam without reinforcement were developed using various guides. As seen from the previous examples with reinforcement the elastic stress vectors indicate the load path splitting around the opening and creating tension above and below. Without reinforcement the concrete is unable to carry a significant load in tension. Reineck (1991) indicated concrete tensile contributions in strut-and-tie models cannot be used to accurately describe ultimate load behavior. Also, once cracking begins any tie would be lost and the entire model would change. For these reasons a model without concrete ties was used to describe the ultimate load state where extensive cracking is present.

A common model was developed to describe each of the three beams. This model is the combination of a left and right load path as shown in Figure 5.3. The

model to the left utilized the perimeter reinforcement to allow a compression strut directed at the left side of the opening. Using the tie on the perimeter allowed a portion of the force to flow towards the left without using a horizontal tie.

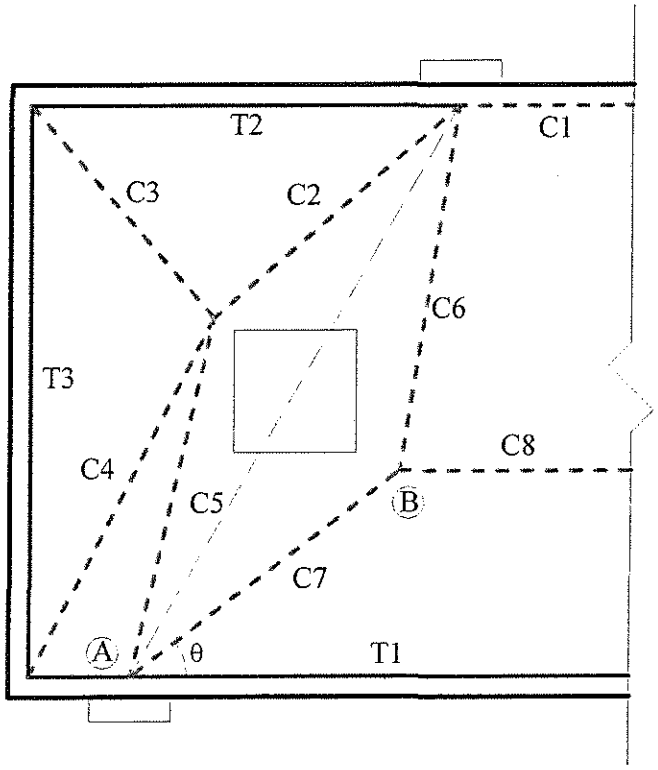

Figure 5.3: Common strut-and-tie model for beams without reinforcement.

The assumption that the vertical ties at the left edge begin to carry load when no significant horizontal reinforcement is provided is supported by comparison of cracking patterns, an elastic finite element analysis, and engineering judgment. Cracking patterns in Figure 5.4 show the presence of tensile cracking at the edge of the beam near the web opening. This is in contrast to Figure 5.5 where beams with adequate horizontal reinforcement do not show any horizontal cracking at the vertical edge near the opening. As well the elastic stress analysis shown in Figure 5.6 gives

some evidence of tensile stress along this edge. This can be explained by the absence of a horizontal tie force causing compression to form an arch and tie mechanism utilizing the vertical perimeter reinforcing bar.

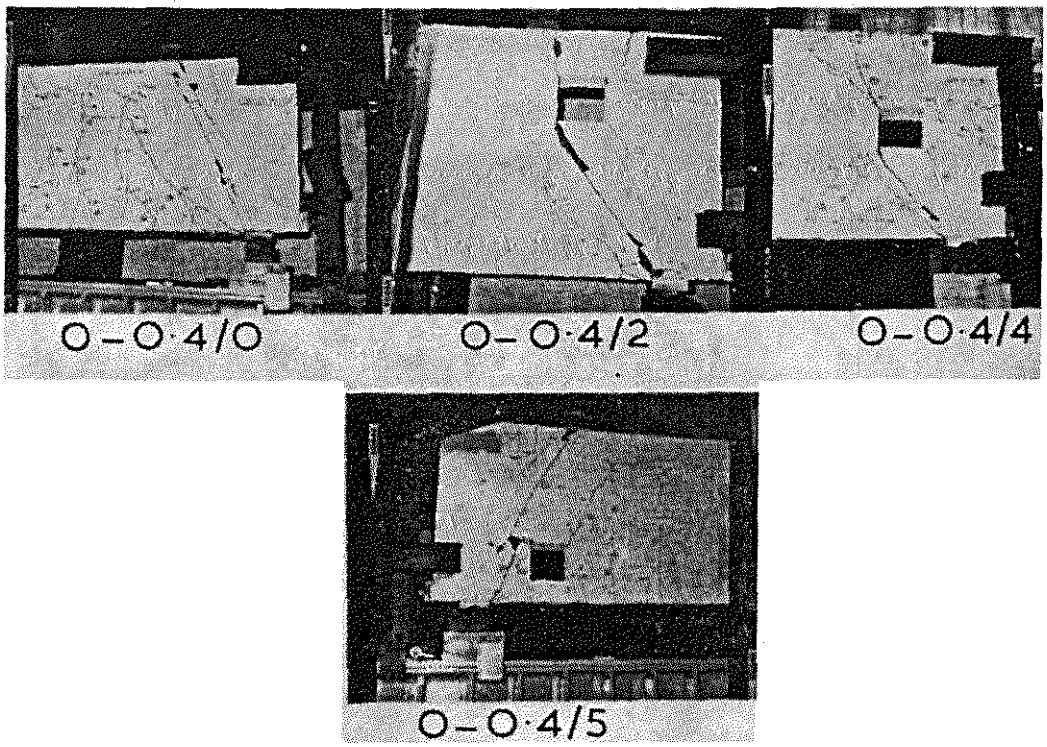

Figure 5.4: Vertical edge cracking patterns for beam without web reinforcement.

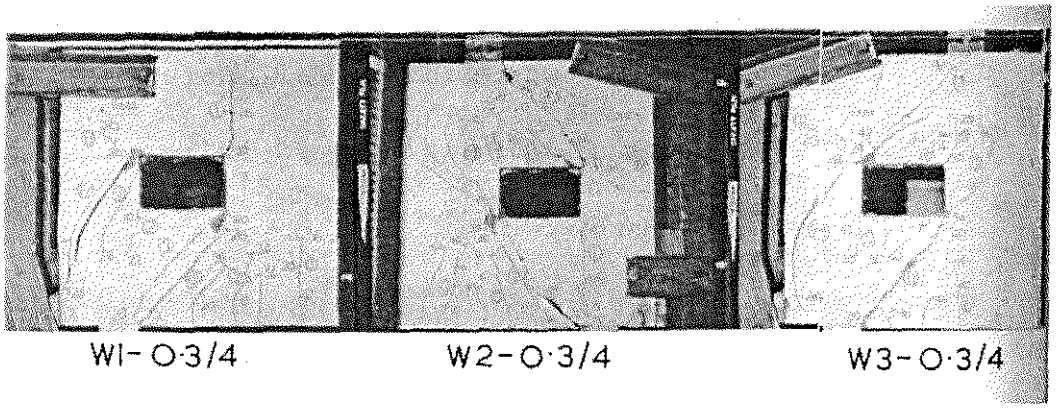

Figure 5.5: Vertical edge cracking patterns for beams with adequate horizontal reinforcement.

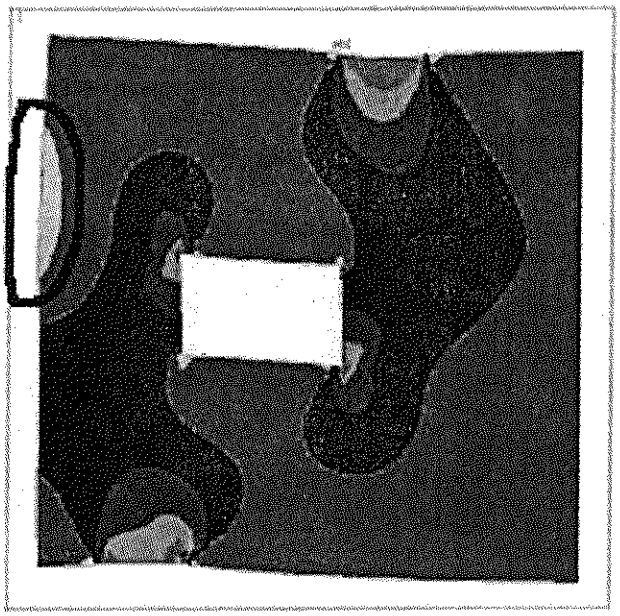

Figure 5.6: Vertical stress contours for W3 (Circled area denotes tension)

The right portion of the model composed of C1, C6 – C8, and T1, utilizes the horizontal strut, C8, directed from the right edge of the opening into the web. Kong (1973) suggested this model in combination with a small tensile path above the opening (Figure 5.7). This model was presented as an idealization of the load path according to the observed behavior and not as a strut-and-tie model. This model is used to describe the increase in beam efficiency as the location of node B approaches the natural load path for a solid beam shown by the dash dot line in Figure 5.3.

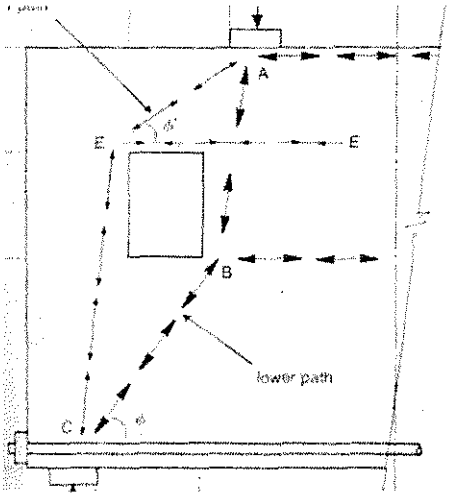

Figure 5.7: Ideal Load path presented by Kong (1973).

5.2 Forces and Ultimate Load Requirements

Calculation of the strut-and-tie forces was done by superposition of truss forces from a combined left and right truss, then from the right truss only composed of C1, T1, C6, C7, and C8 from Figure 5.3. The load, P_l, of the combined truss was calculated when the yield limit of the vertical tie, T3, from Figure 5.3 was reached. The additional load, P_r, was calculated when the right truss reached the strut or tie capacities.

The ultimate load was determined when the total load reached the nodal stress limits, strut stress limits, or the ultimate limit of reinforcement. The nodal stress limits were calculated using the method given in Chapter 3.

A quick simplification of the strut geometry was used to provide only one calculation for strut C7. Since the majority of the load carrying capacity comes from the right side and struts C6 and C7 from Figure 4.3 will be the greatest, nodes A and B are considered to govern strut capacity. θ, from Figure 5.8, was set such that the

stress areas of C7 at the assumed hydrostatic nodes A and B were equal. The area at node B is twice the perpendicular distance to C7 and the area at node A was twice the perpendicular distance from the right support edge to C7. θ is found by setting the equations *a* and *b*, presented in Figure 5.8, equal and solving for θ. With equivalent areas only one node must be checked. The only other checks required are for C6 and the force limitations on the reinforcement.

$$a = (h - x*\tan\theta)*\cos\theta$$

$$b = 25/\cos\theta + \sin\theta*(50 - 25*\tan\theta)$$

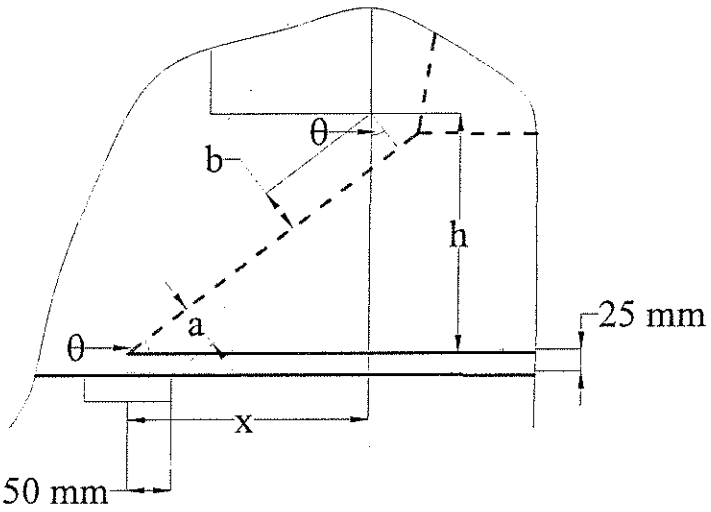

Figure 5.8: Trigonometric relationships for solution of θ.

The reinforcing steel was allowed to surpass the yield stress within reason but not to exceed the ultimate stress. The ultimate stress was determined as 1.5 times the yielding limit:

$f_y = 430$ N/mm^2 (60 ksi)

$f_u = 645$ N/mm^2 (90 ksi)

5.3 Results

The forces for each strut-and-tie truss were quickly calculated using spar elements in the finite element analysis software, Ansys. The results for each model in Figures 5.9 – 5.11 are given in the Tables 5.2 – 5.4. The member forces are given for the combined left-right truss and the separate right truss. In order to express the contribution of each configuration a ratio of load to total load, P_l/P_t and P_r/P_t is given (Table 6.1). The total load predicted using the strut-and-tie model developed is expressed as P_t. This load is then compared to the ultimate load, P_u, found in the tests by Kong (1973) in the ratio P_t/P_u (Table 6.1).

The ultimate loads predicted by the aforementioned empirical equation and from the empirical equation presented in Kong (1973) are shown in Table 5.1. Calculations for the determination of Q_u are given in Appendix B. An excel spreadsheet was used to quickly process each calculation using the simplified design equation from Chapter 1. W_2 was determined in Kong (1973) using a very specific empirical relation developed from the test results.

Table 5.1: Empirically predicted ultimate loads.

Beam	Wu	Qu	Pu
O-0.4/2	191	194.4	185
O-0.4/4	159	187.6	170
O-0.4/5	275	226	270
O-0.4/0	295	319.1	330

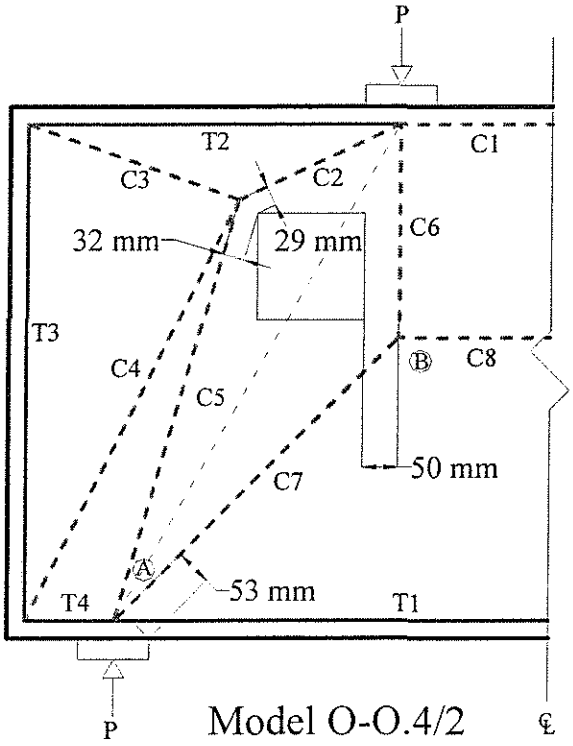

Figure 5.9: Strut-and-tie model for beam O-0.4/2

Table 5.2: Strut and Tie Forces of Model O-0.4/2 at failure.

Combination		Right Side Only		P_t	P_u (Kong)	**P_t/P_u**
Load P_l	P_l/P_t	Load P_r	P_r/P_t	131	185	**0.71**
25	0.19	106	0.81			
Element	Force	Element	Force	Total		
C7	**-24.0**	**C7**	**-150.0**	**-174.0**	**= Strut Limit = 174 kN**	
C6	-16.9	C6	-106.1	-123.0	< Strut Limit = 164 kN	
C8	-16.9	C8	-106.1	-123.0		
C2	-18.1			-18.1		
C3	-12.7			-12.7		
C5	-8.0			-8.0		
C4	-4.8			-4.8		
C1	-4.4	C1	0.0	-4.4		
T1	21.3	T1	106.1	127.4	~ Yield Limit = 134 kN	
T2	12.0			12.0	= Yield Limit = 12 kN	
T3	4.3			4.3		
T4	2.1			2.1		

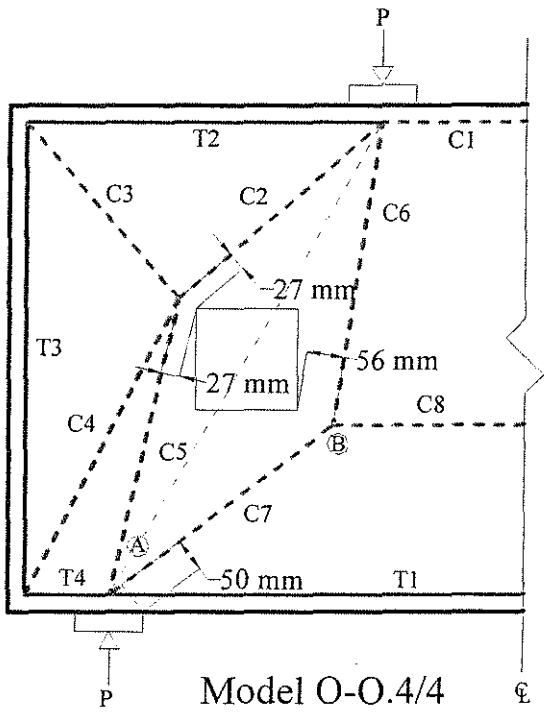

Figure 5.10: Strut-and-tie model for beam O-0.4/4

Table 5.3: Strut-and-tie forces (kN) at failure of Model O-0.4/4

Combination		Right Side Only		P_t	P_u (Kong)	**P_t/P_u**
Load P_l	P_l/P_t	Load P_r	P_r/P_t	118.8	170	**0.7**
33.5	0.28	85.2	0.72			
Element	Force	Element	Force	Total		
C7	**-24.3**	**C7**	**-139.9**	**-164.2**	**= Strut Limit = 164 kN**	
C8	-16.9	C8	-97.3	-114.2		
C6	-15	C6	-86.3	-101.3	<< Strut Limit = 183 kN	
C2	-28.6			-28.6		
C1	-13.1	C1	-13.6	-26.7		
C5	-19.2			-19.2		
C3	-16.7			-16.7		
C4	-14.1			-14.1		
T1	30	T1	110.9	140.9	≥ Yielding	
T3	12.6			12.6	≥ Yielding	
T2	10.9			10.9		
T4	6.4			6.4		

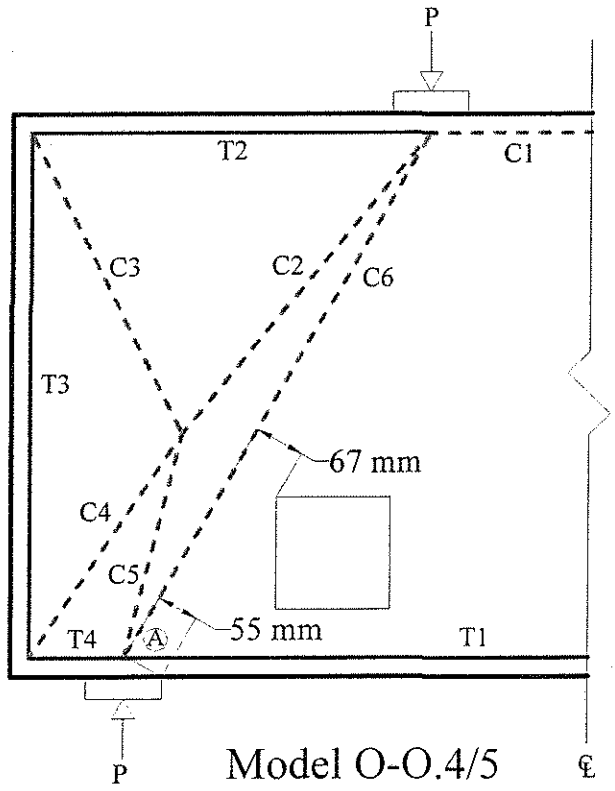

Figure 5.11: Strut –and-tie model for beam O-0.4/5

Table 5.4: Strut-and-tie forces (kN) at failure of Model O-0.4/5

Combination		Right Side Only		P_t	P_u (Kong)	**P_t/P_u**
Load P_l	P_l/P_t	Load P_r	P_r/P_t	188.9	270	**0.7**
63.1	0.33	130.8	0.69			
Element	Force	Element	Force	Total		
C6	-44	C6	-150.7	**-194.7**	**= Strut Limit = 194.7 kN**	
C1	-36	C1	-86.1	-122.1	<< Strut Limit = 178 kN	
C2	-32.1			-32.1		
C5	-25.7			-25.7		
C4	-14.4			-14.4		
C3	-13.4			-13.4		
T1	36	T1	86.1	122.1	<< Yielding	
T3	12			12	= Yielding	
T4	8			8		
T2	6			6		

Chapter 6 Discussion

Consistent results are found for the presented strut-and-tie models applied to deep beams with web openings. For models O-0.4/2, O-0.4/4, and O-0.4/5 the predicted ultimate load was consistently near 70% of the experimental ultimate load. This result also correlates very well with aforementioned experiments run by Maxwell (1996) where the predicted ultimate loads were not as consistent but ranged from 0.56 to 0.71.

The strut-and-tie model correctly reflected reductions in overall strength of the beam, as the location of the opening changed. The model also consistently accounted for an increase in the load carrying efficiency of the left truss configuration. As the opening moves towards the bottom of the beam, the right truss becomes less efficient and load is transferred to the left truss. This is illustrated in Table 6.1, where the percentage of the total load carried by the right truss configuration decreases and the percentage of the total carried by the left truss configuration increases between models O-0.4/2 and O-0.4/4.

Table 6.1: Strut-and-Tie Load Distributions and Predicted/Ultimate Strength

Model	P_l/P_t	P_r/P_t	P_t/P_u	P_u	W_2^*/P_u	Q_u/P_u
O-0.4/2	0.19	0.81	0.71	185	1.04	1.05
O-0.4/4	0.28	0.72	0.70	170	0.93	1.11
O-0.4/5	0.33	0.69	0.70	270	1.02	0.84
O-0.4/0	-	-	0.57	330	0.89	0.96

*W_2 predicted load from Kong (1973)
**Q_u calculated from empirical equation in Chapter 1

Another interesting point is the percentage use of the strut and the tie capacities for each model. In every model presented the capacity of the strut was the governing factor in determining the overall strength. In all but one of these models the horizontal reinforcing steel was pushed up to or near the yield stress. For the beam where the opening did not interfere with a direct load path, model O-0.4/5 (Figure 5.11), the horizontal reinforcing steel was not pushed to the yield limit. This would indicate that as the opening interferes less with a direct load path the common model should be refined to match the change in behavior because similar amounts of cracking were observed at the bottom of all beams. This is supported by the decrease in P_t/P_u ratio to 0.57 for a beam with no web opening, O-0.4/0. For this beam the same ultimate load would be calculated using the model developed for beams with web openings, therefore refinement is suggested in those cases.

Comparison of the empirically predicted load from Kong (1973) and the equation discussed in Chapter 1 is also shown in Table 6.1. This again shows the relative consistency of the strut-and-tie model. The ultimate load ratios of these range from 0.84 to 1.05. Although, the estimates of strength obtained with the empirical equation were closer to the actual ultimate load the accuracy varied depending on the suitability of the beam geometry. Beam O-0.4/5 did not fit one of the shear web criteria and the minimum had to be applied. Q_u is the load calculated from the aforementioned empirical equation and is limited by the beam geometry. This would explain the underestimation of the ultimate load compared with the other predictions. W_2 was a predicted value using an equation proposed by Kong (1973). This equation

gives very close results because it was tailored to the test beams and has two significant limitations:

1) Static top loads are the only valid applied loads.
2) The geometry of the web openings and beams are limited to those used in the test specimens.

In contrast to these limitations strut-and-tie models can be applied to any load situation and beam geometry. Due to these variability and limitations of application, strut-and-tie modeling presents the most consistent and powerful tool to the designer.

Chapter 7 Conclusions

Tests by Maxwell (1996) showed that when the strut-and-tie method is used, the crack pattern and the mode of failure are associated with the choice of model used. The reinforcement layout and node capacity are used to control these two aspects. Contrasting this in the empirical method of design, cracking and ultimate failure can only be predicted by experimental history, not the specific design at hand. With this method, the engineer is limited to the empirical parameters of the opening. The engineer has no real knowledge of the failure mechanism at hand.

In this investigation of strut-and-tie modeling the behavior of beams both with and without reinforcement were consistently related to experimental results and useful adaptations of general models were presented. In beams with horizontal reinforcement a model selected for its overall appropriateness worked very well in predicting the failure load. Unfortunately another useful model utilizing vertical, as well as, horizontal reinforcement could not be presented. For this reason an example is given in Appendix C to illustrate the use of vertical reinforcement in strut-and-tie modeling of deep beams with openings. This example is worked using FIP Recommendations that include similar guidelines to the ACI method.

The examples of beams without reinforcement further illustrate the consistency of strut-and-tie modeling and the use of a general model. The results show that for each model with reduced experimental ultimate loads the predicted load was reduced accordingly. These results also fall within the range of test/estimate ratios obtained by Maxwell (1996).

The strut-and-tie method appears to apply better to beams with web reinforcement than to those without web reinforcement in this study. The ultimate load predicted for beams with reinforcement was 91% of the tested ultimate load. This is 20% better than those without reinforcement. This indicates that the strut-and-tie method is more accurate when tension fields can exist. This is logical since this method is related to elastic analysis, which assumes tension to exist.

Based on the results of this project the recommended reinforcement for beams with web openings is that of the W3 specimen from Kong (1977). Reinforcement should be placed such that tension can be carried above and below the opening as developed from the proper strut-and-tie model. Addition of vertical reinforcement could provide an increase in strength as Kong (1977) indicates. Yet, this assumption is not verified by this study due to the lack of reinforcing details provided, therefore horizontal reinforcement with proper anchorage should be provided.

By using strut-and-tie models the engineer must become familiar with the beam behavior and therefore understand the design task more clearly. This is the classic advantage of strut-and-tie modeling in that the engineer will directly consider reinforcement details, as well as, system behavior.

Chapter 8 Recommendations

The acceptance of strut-and-tie modeling into the structural design field has been a slow process and data to support the method is abundant. The discussion of this paper is specific within this field and there is much less information available. Based on conclusions from this study, the strut-and-tie method provides safe and consistent results for deep beams with web openings. These models also match the work of Maxwell (1996) but the number of comparisons is low. Further work can be done to increase the amount of data to support this. Work could include searching published experiments or by testing new specimens.

Another topic for further work is deep beams with openings with both vertical and horizontal web reinforcement and the corresponding strut-and-tie models. A comparison between beams with both vertical and horizontal web reinforcement versus beams with only horizontal reinforcement would be valuable. This would assess both the fitness of a strut-and-tie model to beam behavior and the optimal reinforcement configuration in design.

It is also recommended to give care in selection of the correct factors in strut capacity. Since every beam in this study is governed by the compression capacity the method from ACI 318 (2002) for calculating the limiting stress of compression struts has a large effect on the overall strength for these beams. In particular the factor for lightweight aggregate given by ACI will have a large impact on the overall capacity in these beams. The correct factor may range from 0.85 to 0.6 and will directly change the predicted ultimate load.

References

American Concrete Institute. (2002). B*uilding Code Requirements For Reinforced Concrete and Commentary*, ACI 318-02, ACI, Detroit.

British Standard Institution. (1972). *The Structural Use of Concrete*, CP110- 72, BSI, London.

Comite Europeen de Beton-Federation Internationale de la Precontrainte. (1970 & 1996). *International Recommendations for the Design and Construction of Concrete Structures*. Cement And Concrete Association, Appendix- 3 London: 17

Kong, F. K., Sharp, G. R. (1973). "Shear strength of lightweight reinforced concrete deep beams with web openings." The Structural Engineer, ASCE, Vol. 51., No. 8, August 1973. pp. 267-275

Kong, F. K., Sharp, G. R. (1977). "Structural Idealization for deep beams with web openings." Magazine of Concrete Research, Vol. 29, No. 99, June 1977pp 81-91

Kong, F. K., (1990). *Reinforced Concrete Deep Beams*. 1st Edition, VanNostrand Reinhold, New York New York.

Maxwell, Brian S., Breen, John E. (1996). "Experimental Evaluation of Strut-and-Tie Model Applied to Deep Beam with Opening." ACI Structural Journal, Vol. 97, No. 1, January-February 2000, pp142-148

Ove Arup and Partners. (1977). *The Design of Deep Beams in Reinforced Concrete*. CIRIA Guide 2, Ove Arup, London.

Reineck, Karl-Heinz (1991). "Ultimate Shear Force of Structural Concrete Members without Transverse Reinforcement Derived from a Mechanical Model." ACI Structural Journal, Vol. 88, No. 5, Septermeber-0ctober 1991 pp 592-602

Schlaich, J., Shafer, K., Jennewein, M. (1987). "Toward a Consistent Design of Structural Concrete." PCI Journal, Vol. 32, No. 3, May/June 1987, pp 74-147

Schlaich, J., Schafer, K., (1991). "Design and detailing of structural concrete using strut-and-tie models." Structural Engineer, Vol. 69, n6, March 19, 1991, pp

Truss Member Force Solutions

Model A

$P := \frac{560}{2}$ $\theta := 74$ $d_1 := 725$ $d_2 := 25$ $Z := d_1 - d_2$ $Z = 700$

$\theta := \text{atand}\left[\frac{(d_1 - d_2)}{325}\right]$ $\theta = 65.095$ $P = 280$

Global System:

$\Sigma M_1 = 0 = P \cdot 325 - T1 \cdot Z$ $T1 = T1 := P \cdot \frac{325}{Z}$ T1 = 130

$\Sigma F_x = 0 = C1 - T1$ $C1 = C1 := -P \cdot \frac{325}{Z}$ C1 = -130

Node A:

$\Sigma F_Y = 0 = C2 \sin\theta = P$ $C2 := \frac{P}{\sin(\theta)}$ C2 = 308.707

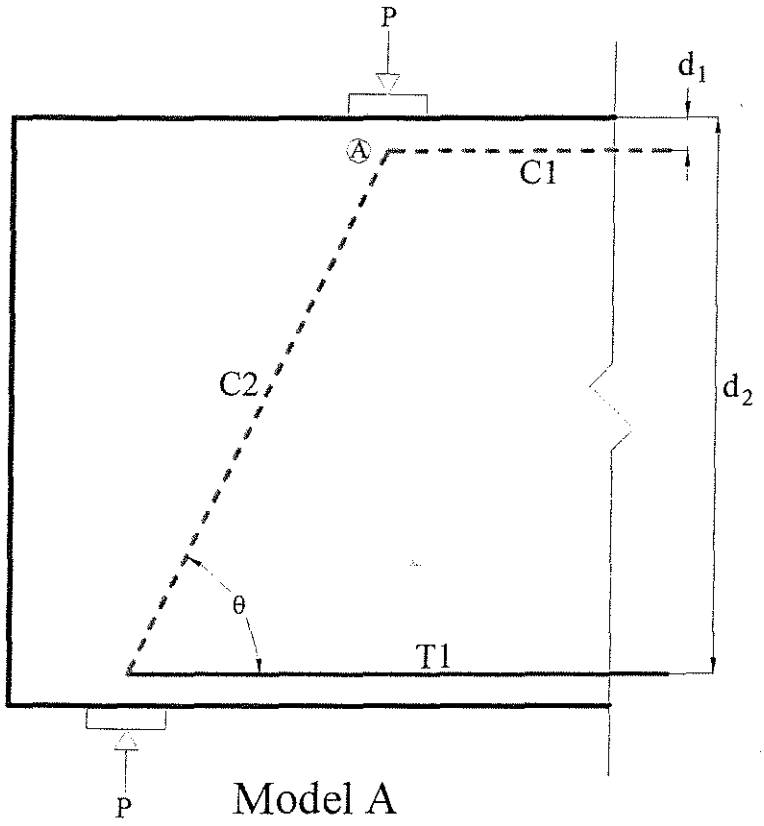

Model A

Model B

$P := 254$

$d_1 := 725 \quad d_2 := 25 \quad d_3 := 275 \quad d_4 := 500 \quad l_1 := 40$

$Z := d_1 - d_2 \quad Z = 700$

$$\theta := \text{atand}\left[\frac{(d_1 - d_2)}{325}\right] \quad \theta = 65.095$$

$$\theta 1 := \text{atand}\left[\frac{(d_3 - d_2)}{\left[275 - l_1 - 2\cdot\left[\frac{(d_3 - d_2)}{\tan(\theta)}\right]\right]}\right] \quad \theta 1 = 89.345$$

$$\theta 2 := \text{atand}\left[\frac{(d_3 - d_2)}{(275 + l_1)}\right] \quad \theta 2 = 38.437$$

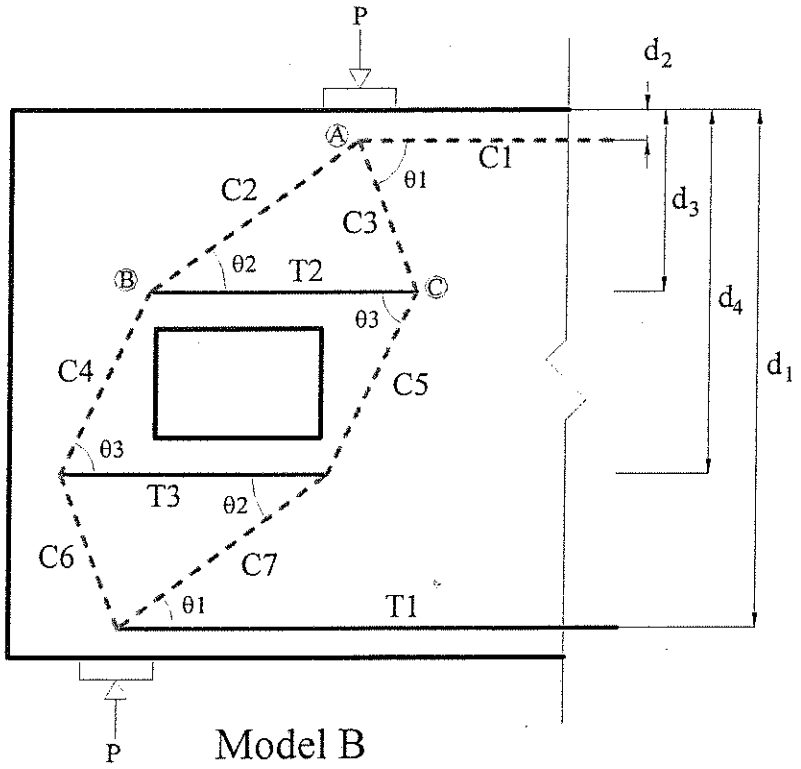

Model B

Global System:

$$T1 := P \cdot \frac{325}{Z} \qquad T1 = 117.929$$

$$C1 := P \cdot \frac{325}{Z} \qquad C1 = 117.929$$

Node A:

$$\Sigma F_x = 0 = -C1 - C3\cos d(\theta 2) + C2\cos d(\theta 2)$$

$$\Sigma F_Y = 0 = -P + C3\sin d(\theta 1) + C2\sin d(\theta 2)$$

Limit C2 = 164

$$C2 := (P + C1 \cdot \tan d(\theta 1)) \cdot \frac{1}{(\cos d(\theta 2)\ \tan d(\theta 1) + \sin d(\theta 2))} \qquad C2 = 152.875$$

$$C3 := \frac{C2 \cdot \cos d(\theta 2) - C1}{\cos d(\theta 1)} \qquad C3 = 158.974$$

Node B:

$$\Sigma F_Y = -C2\sin d(\theta 2) + C4\sin d(\theta 3) = 0$$

Limit C4 = 130

$$C4 := C2 \cdot \left(\frac{\sin d(\theta 2)}{\sin d(\theta)} \right) \qquad C4 = 104.78$$

$$\Sigma F_x = 0 = T2 - C2\cos d(\theta 2) + C4\cos d(\theta)$$

$$T2 := C2 \cdot \cos d(\theta 2) - C4 \cdot \cos d(\theta) \qquad T2 = 75.621$$

Node C:

$$\Sigma F_x = 0 = C3\cos d(\theta 1) - T2 + C5\cos d(\theta)$$

$$C5 := \frac{(T2 - C3 \cdot \cos d(\theta 1))}{\cos d(\theta)} \qquad C5 = 175.262$$

$$\Sigma F_Y := -C3 \cdot \sin d(\theta 1) + C5 \cdot \sin d(\theta)$$

$$\Sigma F_Y = -2.16 \cdot 10^{-12}$$

Model C

Load: $P := 280$

Geometric Layout and Relations:

$d_1 := 725 \quad d_2 := 25 \quad d_3 := 475 \quad l_1 := 200 \quad l_2 := 10 \quad Z := d_1 - d_2$

$$\theta 1 := \text{atand}\left[\frac{(d_3 - d_2)}{l_1}\right] \qquad \theta 1 = 66.038$$

$$\theta 2 := \text{atand}\left[\frac{(d_3 - d_2)}{(275 + l_2)}\right] \qquad \theta 2 = 57.653$$

$$\theta 3 := \text{atand}\left[\frac{(d_1 - d_3)}{(50 - l_2)}\right] \qquad \theta 3 = 80.91$$

$$\theta 4 := \text{atand}\left[\frac{(d_1 - d_3)}{l_1}\right] \qquad \theta 4 = 51.34$$

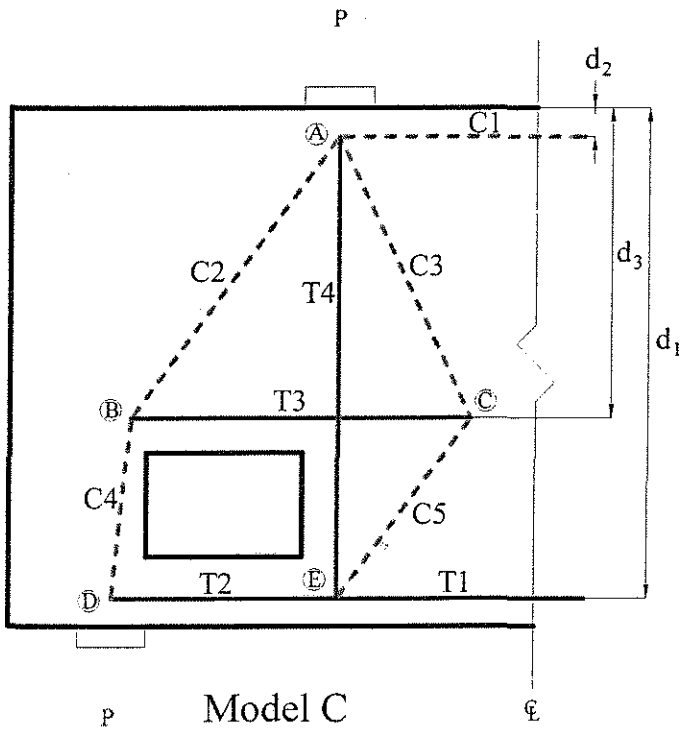

Model C

Global System:

$\Sigma M_1 = 0 = P \cdot 325 - T1 \cdot Z$ $\quad T1 = \quad T1 := P \cdot \frac{325}{Z}$ $\quad T1 = 130$

$\Sigma F_x = 0 = C1 - T1$ $\quad C1 = \quad C1 := P \cdot \frac{325}{Z}$ $\quad C1 = 130$

Node D:

$\Sigma F_Y = 0 = P - C4\,\mathrm{sind}(\theta 3)$

$C4 := \frac{P}{\mathrm{sind}(\theta 3)}$ $\quad C4 = 283.561$

$\Sigma F_X = 0 = T2 - C4\,\mathrm{cosd}(\theta 3)$

$T2 := C4 \cdot \mathrm{cosd}(\theta 3)$ $\quad T2 = 44.8$

Node B:

$\Sigma F_Y = 0 = C4\,\mathrm{sind}(\theta 3) - C2\,\mathrm{sind}(\theta 2)$

$C2 := C4 \cdot \frac{\mathrm{sind}(\theta 3)}{\mathrm{sind}(\theta 2)}$ $\quad C2 = 331.432$

$\Sigma F_X = 0 = C4\,\mathrm{cosd}(\theta 3) + T3 - C2\,\mathrm{cosd}(\theta 2)$

$T3 := -C4 \cdot \mathrm{cosd}(\theta 3) + C2 \cdot \mathrm{cosd}(\theta 2)$ $\quad T3 = 132.533$

Node E:

$\Sigma F_X = 0 = T1 - T2 - C5\,\mathrm{cosd}(\theta 4)$

$C5 := \frac{(T1 - T2)}{\mathrm{cosd}(\theta 4)}$ $\quad C5 = 136.387$

$\Sigma F_Y = 0 = T4 - C5\,\mathrm{sind}(\theta 4)$

$T4 := C5 \cdot \mathrm{sind}(\theta 4)$ $\quad T4 = 106.5$

Node C:

$\Sigma F_Y = 0 = C5\text{sind}(\theta 4) - C3\text{sind}(\theta 1)$

$$C3 := C5 \cdot \frac{\text{sind}(\theta 4)}{\text{sind}(\theta 1)} \qquad C3 = 116.545$$

$\Sigma F_X = 0 = C5\text{cosd}(\theta 4) + C3\text{cosd}(\theta 1) - T3$

$$T3 := C5 \cdot \text{cosd}(\theta 4) + C3 \cdot \text{cosd}(\theta 1) \qquad T3 = 132.533$$

Node A:

$\Sigma F_Y = 0 = C3\text{sind}(\theta 1) + C2\text{sind}(\theta 2) - P$

$$\Sigma F_Y := C3 \cdot \text{sind}(\theta 1) + C2 \cdot \text{sind}(\theta 2) - T4 - P$$

$\Sigma F_Y = 0$

Model D

$P := 560$

$d_1 := 725 \quad d_2 := 25 \quad d_3 := 50 \quad d_4 := 450 \quad Z := d_1 - d_2$

$\theta := \text{atand}\left[\frac{(d_1 - d_2)}{325}\right] \quad \theta = 65.095$

$\theta 1 := 90 - \theta \quad \theta 1 = 24.905$

$\theta 2 := \text{atand}\left(\frac{d_4}{d_3 \cdot \tan(\theta)}\right) \quad \theta 2 = 76.541$

$\theta 3 := \theta - (90 - \theta 2) \quad \theta 3 = 51.637$

$\theta 4 := \theta + (90 - \theta 2) \quad \theta 4 = 78.554$

Global System:

$\Sigma M_1 = 0 = P \cdot 325 - T1 \cdot Z \qquad T1 := P \cdot \frac{325}{Z} \quad T1 = 260$

$\Sigma F_x = 0 = C7 - T1 \qquad C7 := P \cdot \frac{325}{Z} \quad C7 = 260$

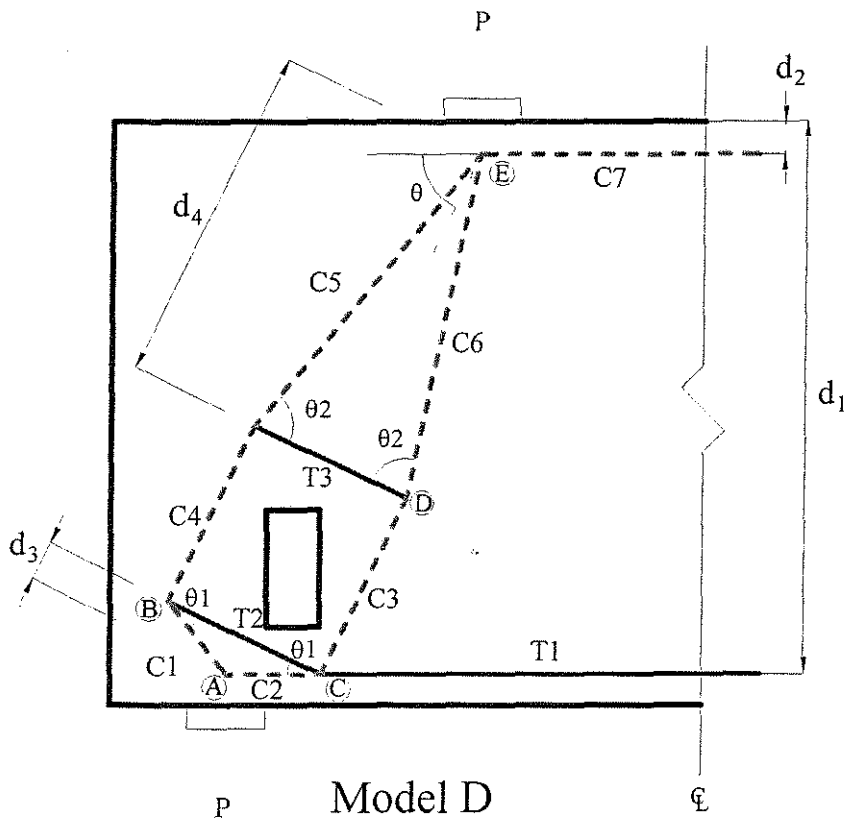

Model D

Node A:

$$\Sigma F_Y = 0 = P - C1\,\text{sind}(180 - 2\theta)$$

$$C1 := \frac{(P)}{\text{sind}(180 - 2\cdot\theta)} \qquad C1 = 733.077$$

$$\Sigma F_X = 0 = C1\,\text{cosd}(180 - 2\theta) - C2$$

$$C2 := C1\cdot\text{cosd}(180 - 2\cdot\theta) \qquad C2 = 473.077$$

Node B:

$$\Sigma F_{C4} = 0 = -C4 + C1\,\text{sind}(\theta 1)$$

$$C4 := C1\cdot\text{sind}(\theta 1) \qquad C4 = 308.707$$

$$\Sigma F_{T2} = 0 = T2 - C1\,\text{cosd}(\theta 1)$$

$$T2 := C1\cdot\text{cosd}(\theta 1) \qquad T2 = 664.907$$

Node C:

$$\Sigma F_Y = 0 = T2\,\text{sind}(\theta 1) - C3\,\text{sind}(\theta)$$

$$C3 := \frac{T2\cdot\text{sind}(\theta 1)}{\text{sind}(\theta)} \qquad C3 = 308.707$$

$$\Sigma F_X = 0 = C2 + T1 - T2\,\text{cosd}(\theta 1) + C3\,\text{cosd}(\theta)$$

$$C3 := \frac{(T1 + C2) - T2\cdot\text{cosd}(\theta 1)}{\text{cosd}(\theta)} \qquad C3 = 308.707$$

Node D:

$$\Sigma F_{C3} = 0 = C3 - C6\,\text{sind}(\theta 2)$$

$$C6 := \frac{C3}{\text{sind}(\theta 2)} \qquad C6 = 317.424$$

$$\Sigma F_{T2} = 0 = T3 - C6\,\text{cosd}(\theta 2)$$

$$T3 := C6\cdot\text{cosd}(\theta 2) \qquad T3 = 73.879$$

$$C5 := C6$$

Node E:

$$\Sigma F_Y = 0 = \quad -P + C5\cdot\text{sind}(\theta 3) + C6\cdot\text{sind}(\theta 4) = -2.274\cdot 10^{-13}$$

$$\Sigma F_X = 0 = \quad C5\cdot\text{cosd}(\theta 3) + C6\cdot\text{cosd}(\theta 4) - C7 = -2.842\cdot 10^{-13}$$

Appendix B

$$\lambda_1 = \left[1 - \frac{1}{3}\left(\frac{K_1 X_N}{K_2 D}\right)\right] \quad for \quad \frac{K_1 X_N}{K_2 D} \le 1$$

$$\lambda_1 = \frac{2}{3} \quad for \quad \frac{K_1 X_N}{K_2 D} \ge 2$$

Beam	K_1	K_2	X_N	D	K_1X_N/K_2D	λ_1
O-0.4/0	1.00	-	400	750	-	1.00
O-0.4/2	0.69	0.70	400	750	0.52	0.83
O-0.4/4	0.50	0.47	400	750	0.57	0.81
O-0.4/5	0.69	0.19	400	750	1.96	0.67

$$\lambda_2 = (1 - m)$$

Beam	m	λ_2
O-0.4/0	0.00	1.00
O-0.4/2	0.21	0.79
O-0.4/4	0.20	0.80
O-0.4/5	0.00	1.00

$$\lambda_3 = \left[0.85 \pm 0.3\left(\frac{e_S}{X_{net}}\right)\right]\left[0.85 \pm 0.3\left(\frac{e_e}{Y_{net}}\right)\right]$$

$e_S \le X_N / 4 \quad e_Y \le 0.6D / 4$

$X_{net} = (X_N - a_1 x) \quad Y_{net} = (0.6D - a_2 D)$

Beam	e_X	$< X_N/4$	e_Y	0.6D/4	a_1	a_2	X	X_{NET}	Y_{NET}	λ_3
O-0.4/0	-		-		0	0	300	400	450	1
O-0.4/2	-75	100	150	112.5	0.5	0.2	300	250	300	0.76
O-0.4/4	0	100	0	112.5	0.5	0.2	300	250	300	0.723
O-0.4/5	75	100	135	112.5	0.5	0.2	300	250	300	0.926

$$Q_u = \left[0.1 f_c'(\lambda_1 \times \lambda_2 \times \lambda_3) + 0.0085 \psi_s p_s f_{sy}\right] \times bD$$

$$Q_u = \left[F_C + F_S\right] \times bD$$

Beam	l1	l2	l3	f'c	FC	FS	**Qu**
O-0.4/0	1.00	1.00	1.00	32.6	3.26	1.00	**319.1**
O-0.4/2	0.83	0.79	0.76	32.4	1.60	1.00	**194.4**
O-0.4/4	0.81	0.80	0.72	32.2	1.51	1.00	**187.6**
O-0.4/5	0.67	1.00	0.93	32.7	2.02	1.00	**226.0**

Deep Beam with Opening Using Vertical and Horizontal Reinforcement

The deep beam with an opening in the middle is designed using FIP Recommendations 1996. The given load is design value.

Materials:

Concrete C 30/37 [corresponding to f'_c28.4 Mpa = 4,119 psi]

Steel S500 f_{yk} = 500 Mpa [characeristic yield strength of 72,500 psi]

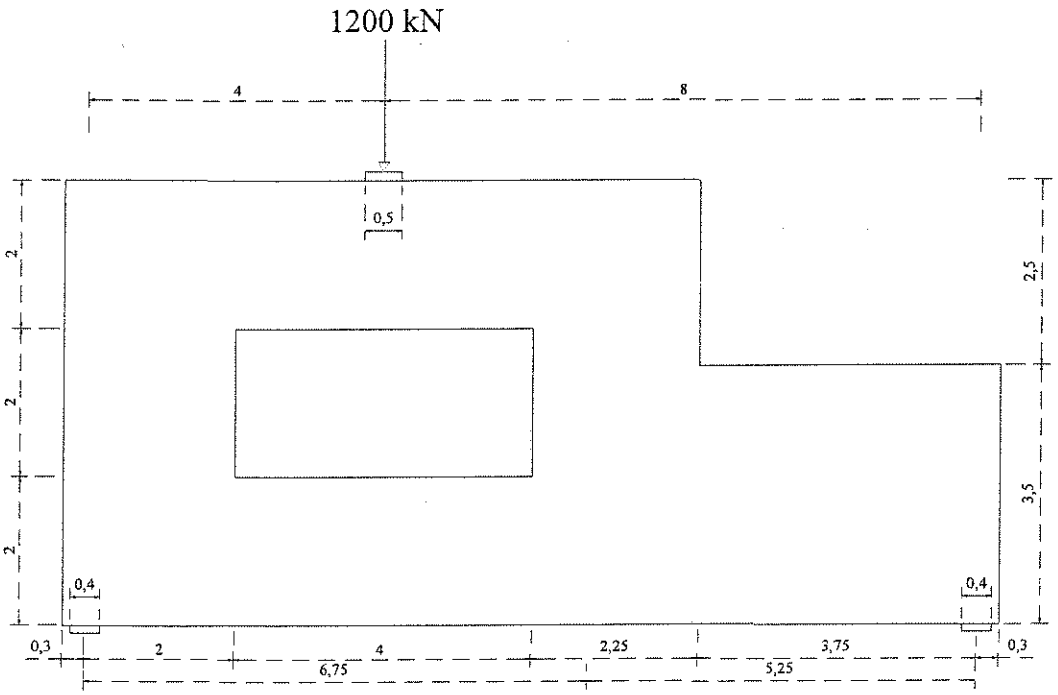

C.1 Model variations

Model A1: "Simply supported"

The simplest model is that the upper section above the opening acts as a simply supported beam with supports 0.75 m beyond the opening edge (Figure C.1). The lower part below the opening is assumed to act as a simply supported beam loaded by the reactions from the upper beam. Fig. 1.1 shows the statical system and Fig. C.2 gives a strut-and-tie model.

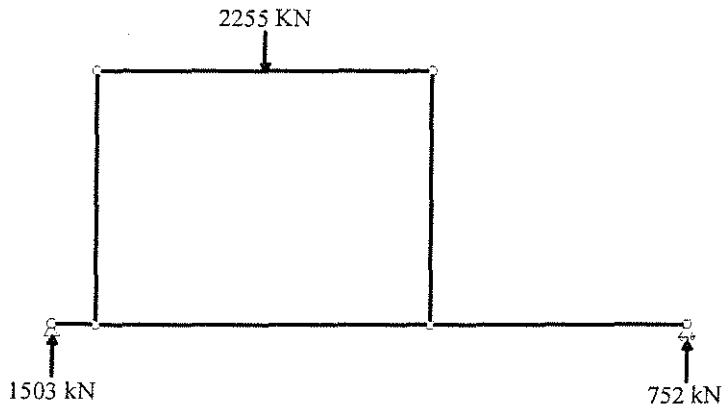

Figure C.1: Representation of simply supported beam system

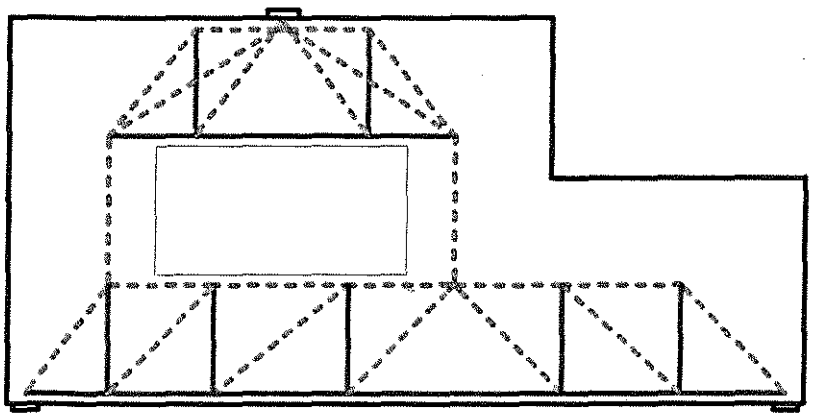

Figure C.2: A1 strut-and-tie model

Model A2: "Fixed end beam"

The same system of upper and lower beams continues with a variation. In this case the upper beam is modeled as a fixed end beam. This recognizes the potential for tensile stresses in both the central section above the opening and in the upper corner regions of the upper beam (see Figure C.3 and C.4). The lower beam is then a simply supported beam which carries the vertical forces and resulting moments from the upper part of the structure.

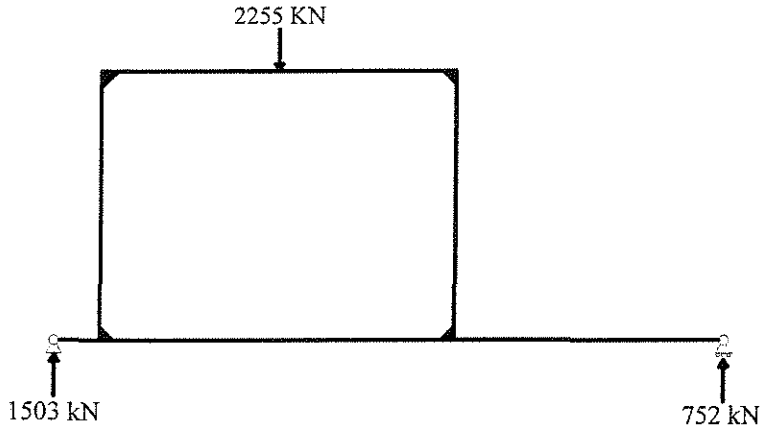

Figure C.3: Representation of clamped end beam

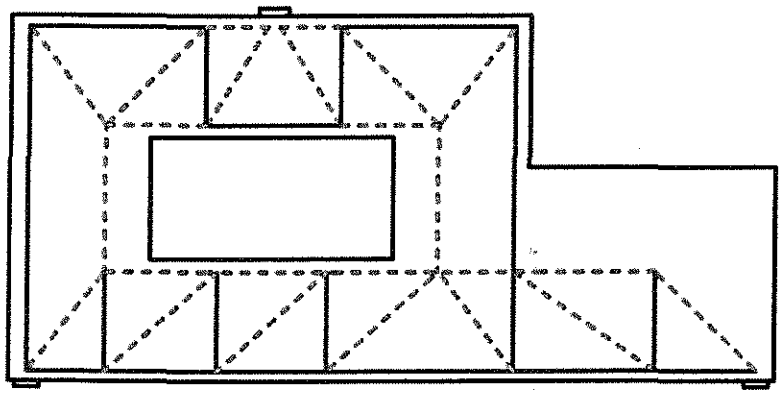

Figure C.4: A3 strut-and-tie model

Model A3: "Corbel action upper beam"

According to the plasticity theory it is also possible that the moment in the middle region is chosen as zero. The upper beam is then split into two cantilevered beams or corbels considering the dimensions. Each will carry half the load to the lower simple beam (see Figure C.5). The resulting strut-and-tie model is shown in Figure C.6.

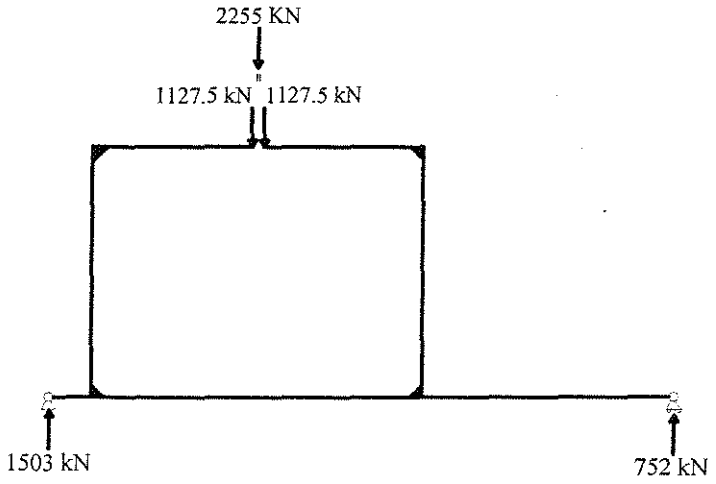

Figure C.5: Corbel system

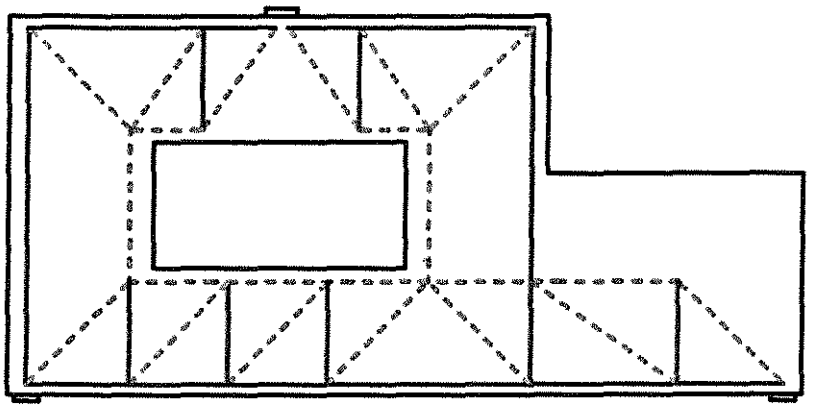

Figure C.6: A2 strut-and-tie model

C.2 Results of finite element analysis

With finite element analysis the linear-elastic behavior of the deep beam can be observed. This portrays the load paths and areas where tension or compression become most important. The results of the elastic analysis shown in Figure C.7. The main tensile areas are found in the regions above the opening and along the bottom of the deep beam. This is exactly as assumed in Model A1. It is apparent that almost no tensile forces are found elsewhere. With exception, a minimal amount of tensile stresses can be found on the outer edge of the upper left deep beam area.

This analysis adds insight to the initially chosen models in comparison of the flow of forces or "load paths". It is worthwhile to notice the flow of forces from the upper region to the bottom supports (see Figure C.7). The compression vectors display a much more direct flow towards the supports from the regions at the upper corners of the opening. This is in contrast to the original models, which used simplified vertical struts. The vertical struts from model A1 shall be replaced by the inclined ones. This will reduce the amount of tension in the upper region as well better approximate the load paths.

Figure C.7 also displays a concentration of the compression at the upper corners of the opening. One change not made in the new model is to move the upper nodes of the struts closer to these corners. While this reduces the tension in the upper beam it is not advisable to place the nodes closer to the edge due to stress and cover allowances.

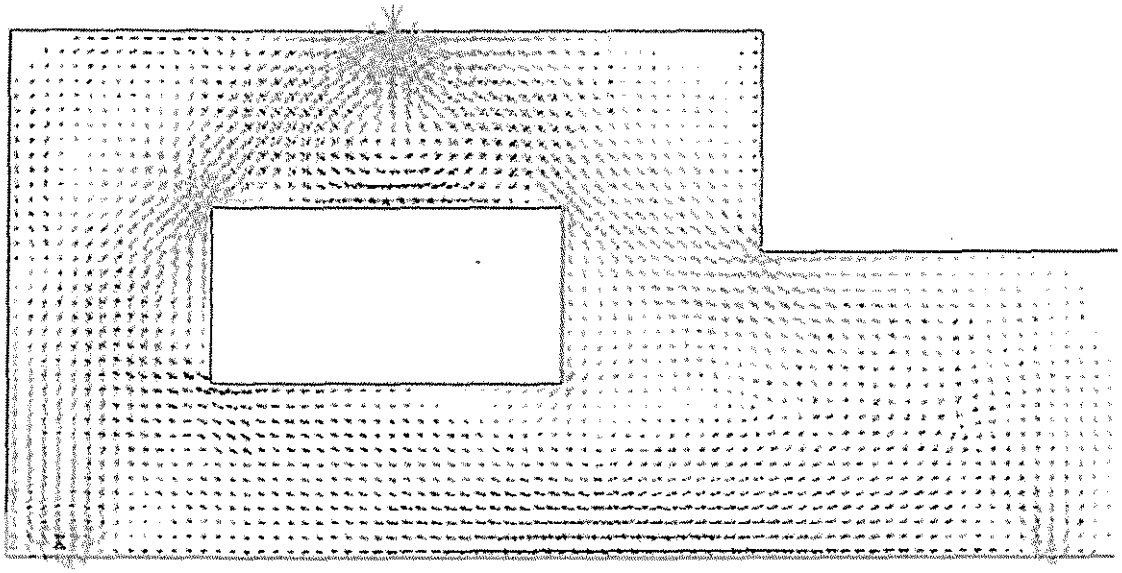

Figure C.7: Elastic stress vectors for example beam.

C.3 Refined Model A1 and Design

Model refinements

A strut directly from Node C to F and a complementary system from Node B to D (see Figure C.8) replace the previous vertical strut system. A way for realizing this refinement and keeping equilibrium is through superposition to previous models. Due to symmetry it is required to keep a vertical strut on the right hand side. This provides equilibrium between C1, C2, C3, and the upper beam. Through inclined struts tension in T1 is reduced and transferred to T2 while the direct compression field is accounted for. As a whole this refinement provides for more realistic portrayal of elastic forces shown in the FEA.. When the model is deemed refined and complete for design purposes the constructive detail calculation and reinforcement layout is set upon. Since the refinement of Model C follows the principles of Load path design and better approximates the behavior shown in elastic anlysis it is chosen for the final model.

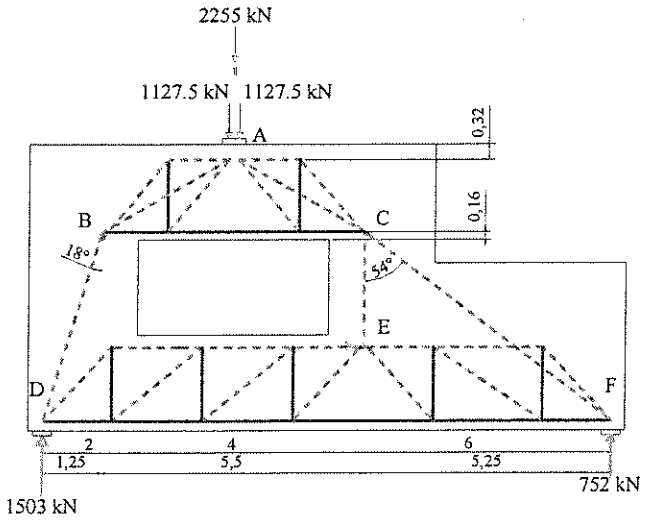

Figure C.8: Refined version of A1 strut-and-tie model

Factored Loads

The factored beam weight is applied at the single upper loading point.

Self Weight $G = (6 \cdot 12 - 4 \cdot 2 - 4.05 \cdot 2.5)0.25 \cdot 25 kN/m^3 = 337$ kN

$\gamma_g \cdot G + \gamma_q \cdot Q_1 = 1.35(337) + 1.5(1200) = 2255$ kN

Design values

$f_{cd} = \alpha \cdot f_{ck} / \gamma_c = 0.85(50)/1.5 = 28.3$ MPa

$1.2\ f_{cd} = 34$ MPa

$f_{yd} = f_{yk} / \gamma_s = 500 / 1.15 = 435$ MPa

$f_{ctm} = 0.30 \cdot f_{ck}^{\wedge (2/3)} = 4.07$ MPa

Force and reinforcement calculations

$T1 = 2200(2.75 / 1.52) - 2200 \cdot \tan 18 = 3625.4$ kN

$A_{s\ req.} = 3625.4 / 0.435 = 8334\ mm^2$

$A_{s\ prov.} = 8483\ mm^2 \rightarrow 27\ Ø\ 20$

$T2 = M / z + \sin 18 \cdot C1$

$M/z = [C2 \cdot (6.75 / 12) \cdot 5.25] / 1.54 = 2332.4$

$C1 \cdot \sin 18 = 2313.2 \cdot 0.31 = 714.8$

$T2 = 2332.4 + 714.8 = 3047.2$ kN

$A_s = 3047.2 / 0.435$ MPa $= 7005\ mm^2$

$A_{s\ prov.} = 7540\ mm^2 \rightarrow 24\ Ø\ 20$

Upper beam vertical reinforcement requirements:

T5 is found through following equation taken the from FIP Recommendations

$$T5 = F_w = F \cdot (2(a/z) - 1)/ 3$$

$$T5 = 2200 \cdot (2(2.75/ 1.52)-1)/ 3 = 1920.2 \text{ kN}$$

$$A_{s\ req.} = 1290.2/ 0.435 = 4414 \text{ mm}^2$$

$$A_{s\ prov.} = Ø\ 14\ @\ 66 \text{ mm} = 4617 \text{ mm}^2$$

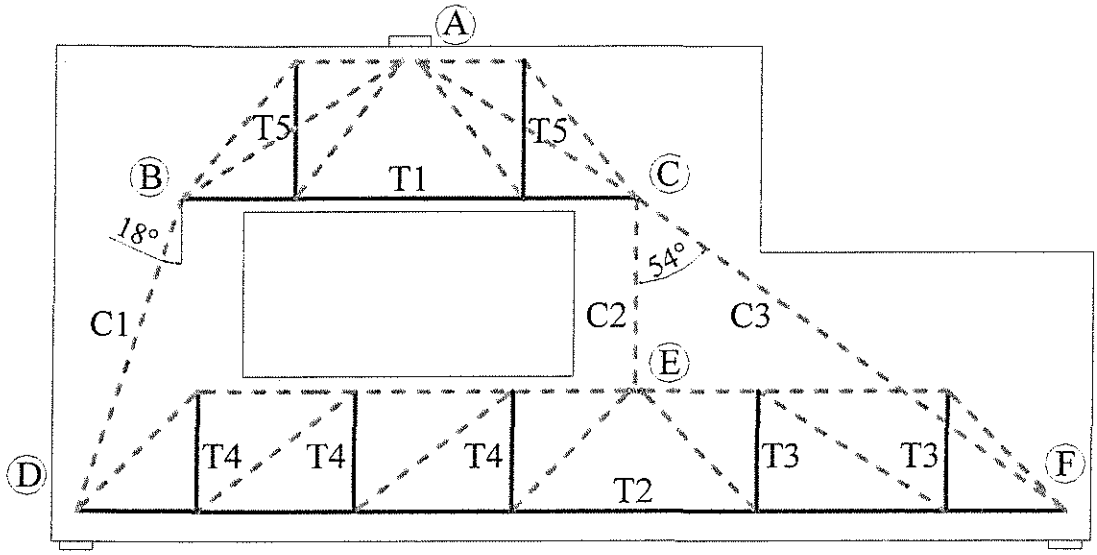

Table C. 1 Strut-and-tie forces

Tie	Tension (kN)	Strut	Compression (kN)
T1	3625.4	C1	2313.2
T2	3047.2	C2	1216.3
T3	684.2	C3	1216.1
T4	532.1		
T5	1920.2		

Preliminary nodal checks

Nodal calculations are made to consider the required strength where the struts and ties met. Adequate area of concrete with respect to stress distribution inside design limitations must be allowed. Likewise adequate development lengths for tension reinforcement must be provided.

The placement of both the upper horizontal struts and the horizontal ties were set in consideration of the assumed $M \cdot z = 0.9d$, allowable compression stresses and FIP recommendations for distribution of tensile reinforcement along the bottom of wall designs. Labeling for the final strut-and-tie model can be found in Figure. C.8. The following are typical calculations for the allowable stress and anchorage.

Compression struts: – see Table 5.2 for ocmpression at Node A

Node E

$$\sigma_{co} = 3.63MN/[(.32\text{-}0.035) \cdot 2 \cdot (0.3 \cdot 0.07)] = 27.7 \text{ Mpa} < 1.2f_{cd} = 34$$

Anchorage length:

$l_b = \varnothing f_{yd}/ (4f_{bd})$ from Table 2.5 FIP $l_b/ \varnothing = 36.2$

$l_b = 36.2 \cdot 20 \text{ mm} = 724 \text{ mm}$

$l_{b \text{ net.}} = \alpha \cdot l_b \cdot (A_{s \text{ req}}/ A_{sprov})$

for hooked bars $l_{b \text{ net.}} = 0.7 \cdot 724 = 507$ mm

thus providing 15% more reinforcement than required will provide an anchorage length under than the maximum available

$l_{b \text{ avail.}} \leq 500 - 2 \cdot 35 = 430$ mm

Shear Design Methods Using Strut-and-Tie Models

With use of strut-and-tie models a discrepancy arises in shear design. The discrepancy is found if the diagonal shear struts of a B-region are set at specific angles with a set number of nodes or a left as a stress field with no predetermined nodes in which the strut angle can later be determined by selection or by force calculations. Fig C.8 and C.9 compare these differing representations. Both modeling techniques will provide a sound design yet predetermined angle selection can lead to awkward angle selections in order to use the closed frame system and thus it is not the most economical reinforcement plan and will not be used.

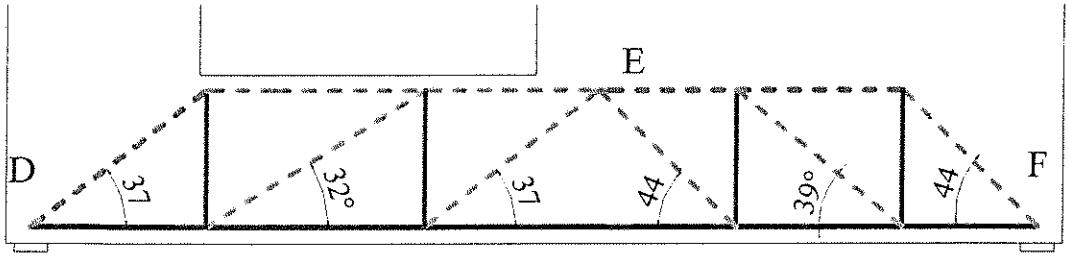

Figure C.8: Closed strut-and-tie model

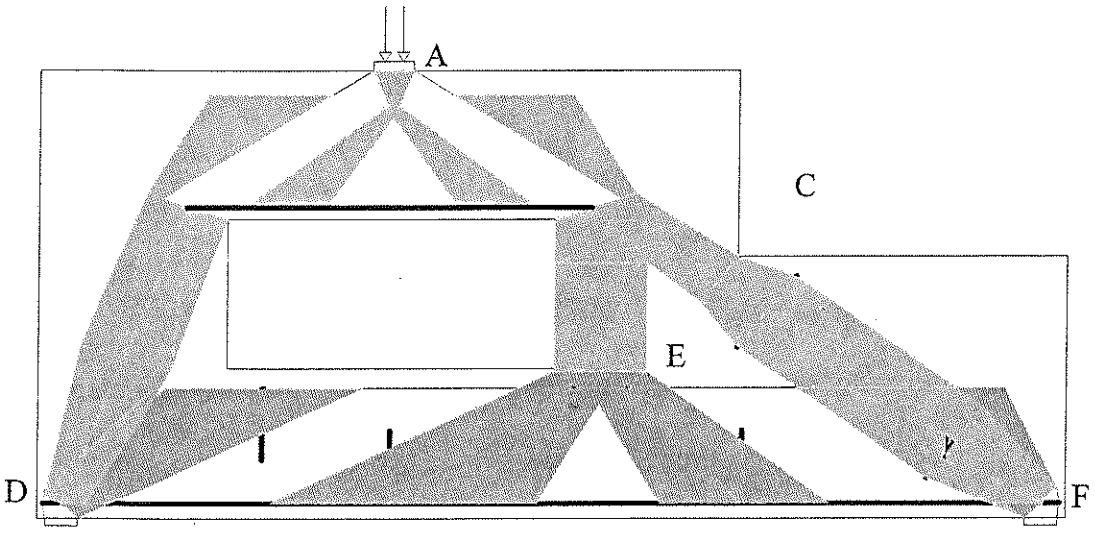

Figure C.9: Open strut-and-tie model

Open shear design

Find required stirrups for T4:

$V_{sd} - V_{fd} = V_{swd}$

$V_{sd} = 532.1$ kN

$V_{fd} = 0.070\ (b_{wz}\ z\ f_{cwd})$

$= 0.070\ (230 \cdot 1540 \cdot 0.8 \cdot 0.0204) = 405$

$A_{sw}/\ s = V_{swd}/\ f_{ywd} \cdot z \cdot \cot\beta_r$

$f_y = 0.435$ kN/mm^2; $z = 1.540$ m; $\cot\beta_r = 1.2$

$A_{sw}/\ s = (532.1 - 405)/\ (0.435 \cdot 1.54 \cdot 1.2)$

$= 158$ mm^2/m

Minimum Requirement:

$A_{s\ min} = 0.1\% \cdot$ Cross Section

$= 0.001 \cdot 300$ mm $= 300$ mm^2/m

or

$A_{sw,\ min}/\ s_w = 0.2\ b_w\ s_w \sin(\theta)\ f_{ctm}/\ f_{yk}$

$= 0.2 \cdot 230 \cdot 1000 \cdot \sin 23.2 \cdot (4.07/\ 500) =$ 148 mm^2/m

choose $A_s > 300$ mm^2: 6 Ø6/m $A_{sw}/\ s = 340$ mm^2/m

Find θ:

$\cot\theta = V_{sd} / [(A_{sw} / s_w)\ f_{ywd}\ z]$

$= 532.1$ kN $/ [(340)\ 0.435 \cdot 1.54]$

$= 2.34$

$\theta = 23.2°$

Required end reinforcement:

Now that the strut angle is determined the end support angle for D-region calculations can be determined.

$$\cot\theta_a = \left[\frac{1}{2}\frac{a_1}{z} + \left(\frac{d_1}{z} + \frac{1}{2}\right)\cot\theta\right]$$

$$\cot\theta_a = \left[\frac{1}{2}\frac{0.4}{1.54} + \left(\frac{0.36}{1.54} + \frac{1}{2}\right)\cot 23.2\right] = 1.84 \Rightarrow \theta = 28.5$$

The tension force for anchorage in node D can be calculated by summing the result from eqn 6.31 of FIP Recom. and the horizontal force from strut C1:

$F_{sA} = V \cdot \cot\theta + C1 \cdot \sin 18°$

$F_{sA} = 532.1 \cdot 1.84 + 2313 \cdot \sin 18° = 1693.8$ kN

$A_s = 1693.8/0.435 = 3894$ mm^2

Find minimum $A_{s\ prov.}$ Of(using hooked end reinforcement see Fig. 2.14):

$l_{b\ net} = 0.7 \cdot (36.2 \cdot 20) \cdot (3894/ A_{s\ prov.}) = 430$ mm

$A_{s\ prov.} > 4589$ mm^2

choose end reinforcement of: 16 Ø20 $\rightarrow$ $A_{s\ prov.} = 5024$ mm^2

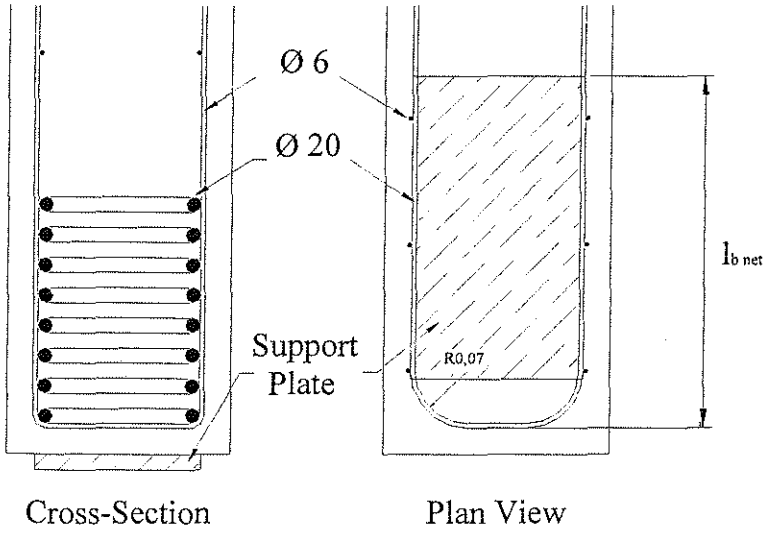

Figure C.10: Reinforcement Detail Node D

Open shear design for T3

For simplification of detailing the end beam tension Fs in the D-regions at Node D and F can be kept equal. Therefore the reinforcement layout is the same. Thus for the shear design chose an angle greater than 23. Choose thirty or it can be back calculated to find that q >25 will provide for equal or less value of Fs. Choose q = 25.

Stirrups required for θ:

$$\cot \theta = V_{sd} / [(A_{sw} / s_w) f_{ywd} z]$$

$$A_{sw} / s_w = V_{sd} / [\cot \theta f_{ywd} z]$$

$$= 684 \text{ kN} / [(1.54) \cdot 0.435 \cdot 1.54]$$

$$= 663 \text{ mm}^2/\text{m}$$

Stirrups required for carrying shear force:

$V_{sd} - V_{fd} = V_{swd}$

$A_{sw}/ s = V_{swd}/ f_{ywd} \cdot z \cdot \cot\beta_r$

$V_{sd} = 0.684$ MN

$V_{fd} = 0.070 (b_{wz} z f_{cwd})$

$= 0.070 (0.23 \cdot 1.54 \cdot 0.8 \cdot 20.4) = 0.405$

$f_y = 0.435$; $z = 1.54$ m; $\cot\beta_r = 1.2$

$A_{sw}/ s = (684 - 405 \text{ kN})/ (0.435 \cdot 1.54 \cdot 1.2)$

$= 347 \text{ mm}^2/\text{m}$

choose stirrups: 7 Ø8/m $A_{sw}/ s = 804 \text{ mm}^2/\text{m}$

Check θ:

$\cot\theta = V_{sd} / [(A_{sw} / s_w) f_{ywd} z]$

$= 684 \text{ kN}/ [(804) 0.435 \cdot 1.54]$

$= 1.27 \rightarrow \theta = 38.2$

Minimum Requirement:

$A_{sw, min}/ s_w = 0.2 b_w s_w \sin(\theta) f_{ctm}/ f_{yk}$

$= 0.2 \cdot 230 \cdot 1000 \cdot \sin 38.2 \cdot (4.07/ 500) = 232 \text{ mm}^2/\text{m}$

or 300 mm^2/m

chosen reinforcement is adequate.

Determine the end support angle for D-region.

$$\cot\theta_a = \left[\frac{1}{2}\frac{a_1}{z} + \left(\frac{d_1}{z} + \frac{1}{2}\right)\cot\theta\right]$$

$$\cot\theta_a = \left[\frac{1}{2}\frac{0.4}{1.54} + \left(\frac{0.36}{1.54} + \frac{1}{2}\right)\cot 38.2\right] = 1.06 \Rightarrow \theta = 43.2$$

The end beam tension force at node F can be calculated by summing the result from eqn 6.31 of FIP Recommendations and the horizontal force from strut C3:

$F_{sA} = V \cdot \cot\theta + C3 \cdot \sin 54°$

$F_{sA} = 684 \cdot 1.06 + 1216.1 \cdot \sin 54° = 1709$ kN

$A_s = 1709/0.435 = 3928$ mm^2

$A_{s\ prov.} = 5024$ mm^2 $\rightarrow$ 16 Ø 20

This gives a resulting anchorage length of:

$l_{b\ net} = 0.7 \cdot (36.2 \cdot 20) \cdot (3928/5024) = 396$ mm

$l_{b\ net.} < l_{b\ prov.}$

396 mm < 430 mm

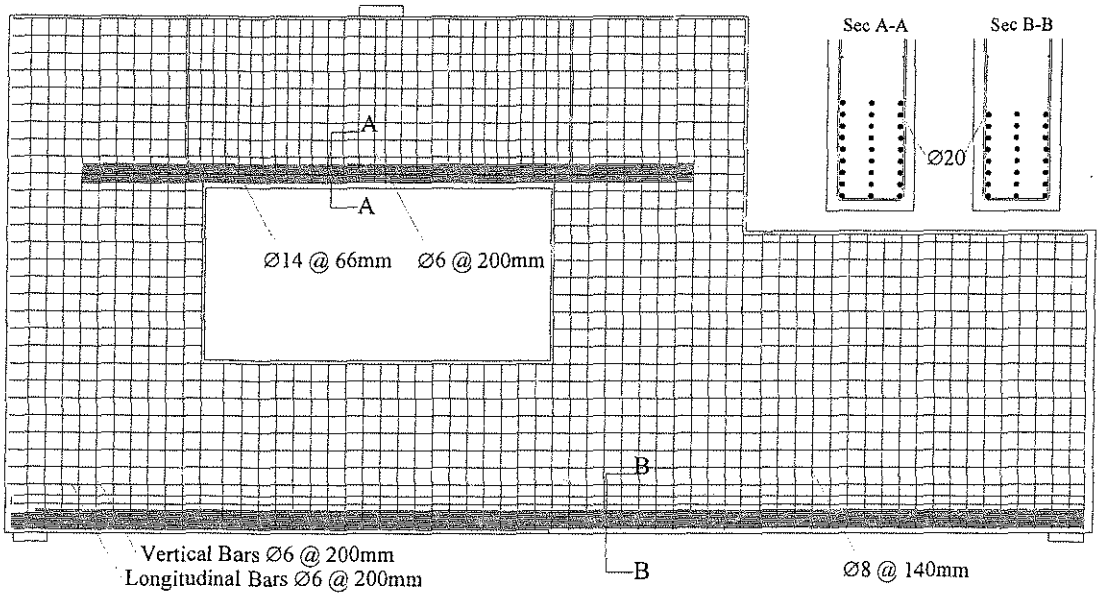

Figure C.11 Reinforcement layout